International Journal of Pharmaceutics 676 (2025) 125581

Contents lists available at ScienceDirect

International Journal of Pharmaceutics

journal homepage: www.elsevier.com/locate/ijpharm

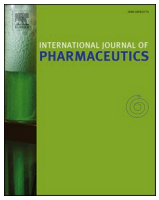

Clinical implementation of a paediatric 3D-printed combination of Sulfamethoxazole and Trimethoprim

Maxime Stoops [a,*], Bernard Do [a,b], Stéphanie Ramos [a], Bing Xun Tan [c], Nicholas Yong Sheng Chua [c], Roseline Mazet [d], Nicolas Guiblin [e], Alexandre Michelet [f], Stephen Flynn [g], Samuel Abbou [h,i], Alvaro Goyanes [j,k], André Rieutord [a], François-Xavier Legrand [l], Maxime Annereau [a,*]

[a] Clinical Pharmacy Department, Gustave Roussy Cancer Campus, 94800 Villejuif, France
[b] Université Paris-Saclay, CNRS, Institut des Sciences Moléculaires d'Orsay, 91405 Orsay, France
[c] Roquette Asia Pacific Pte. Ltd., 11 Biopolis Way, #05-06 Helios 138667, Singapore
[d] CHU Grenoble Alpes, Department of Pharmacy, University Grenoble Alpes, 38700 Grenoble, France
[e] Université Paris-Saclay, CentraleSupélec, CNRS, Laboratoire SPMS, 91190 Gif-sur-Yvette, France
[f] Applications Development Lab France, PerkinElmer, Les Algorithmes - Bâtiment Esope, route de l'Orme des Merisiers, 91190 Saint-Aubin, France
[g] Roquette Frères, 101 Av. de la République, 59110 La Madeleine, France
[h] Children and Adolescent Oncology Department, Gustave Roussy Cancer Campus, 94800 Villejuif, France
[i] Université Paris-Saclay, Institut Gustave Roussy, Inserm, Immunologie anti-tumorale et immunothérapie des cancers, 94805 Villejuif, France
[j] Departamento de Farmacología, Farmacia y Tecnología Farmacéutica, I+D Farma (GI-1645), Facultad de Farmacia, Instituto de Materiales (iMATUS) and Health Research Institute of Santiago de Compostela (IDIS), Universidade de Santiago de Compostela 15782 Santiago de Compostela, Spain
[k] Department of Pharmaceutics, UCL School of Pharmacy, University College London, 29-39 Brunswick Square, London WC1N 1AX, UK
[l] Université Paris-Saclay, CNRS, Institut Galien Paris-Saclay, 91400 Orsay, France

ARTICLE INFO

Keywords:
3D Printing
Paediatric Medicine
Personalized Drug Delivery
Semi-Solid Extrusion (SSE)
Infrared Hyperspectral Imaging (IHI)

ABSTRACT

Adherence to treatment is one of the major challenges in chronic diseases. Inappropriate dosage forms or bad taste are the main factor for non-adherence, especially in paediatric patients. 3D printed medicines could be tailored to specific patients to make medicines more acceptable, however the clinical implementation in hospitals is still limited. This study addresses the challenge of developing pharma-inks (mixtures of drugs and excipients) for semi-solid extrusion (SSE) to produce chewable tablets of Sulfamethoxazole (SMX) and Trimethoprim (TMP) for paediatric oncology patients in a hospital setting. SMX and TMP pharma-inks were stable and printable on demand for more than 3 months. The chewable tablets were also stable, and the drug dissolution profiles were comparable to those of the commercial formulations, indicating potential bioequivalence. Human sensory evaluations confirmed that the formulation improved palatability compared to traditional suspensions. 3D-printed SMX/TMP formulations are an alternative to traditional formulations for paediatric patients in hospital settings, enhancing acceptability and adherence while enabling personalized dosing.

1. Introduction

The treatment of young patients in hospital settings presents unique challenges, especially with regards to dose personalization and medication acceptability. Paediatric patients, particularly those in oncology, often require medication formulations that are not only appropriately dosed but also palatable to ensure adherence and maximize therapeutic efficacy. For antibiotics like Sulfamethoxazole and Trimethoprim (SMX/TMP), commonly used for prophylaxis and treatment in children (Gillet et al., 2023; Madhi et al., 2023; Mattoo et al., 2021; Nelson et al., 2016; The RIVUR Trial Investigators, 2014; ESPGHAN, 2014), adherence is often compromised due to unappealing formulations (Baguley et al., 2012; Kardas et al., 2021). Current oral dosage forms, such as tablets and suspensions, pose significant challenges: tablets are frequently difficult to swallow for children, and the bitter taste of suspensions often leads to refusal, undermining treatment efficacy (Piana et al., 2017; Romandini et al., 2021; Santer et al., 2014; WHO, 2014). Paediatric patients, who are particularly sensitive to bitterness and generally prefer sweet

* Corresponding authors.
E-mail addresses: mstoops@chu-grenoble.fr (M. Stoops), maxime.annereau@gustaveroussy.fr (M. Annereau).

https://doi.org/10.1016/j.ijpharm.2025.125581
Received 4 February 2025; Received in revised form 6 April 2025; Accepted 7 April 2025
Available online 17 April 2025

flavours, are disproportionately affected by these issues, complicating the administration of SMX/TMP and similar medications (Mennella and Bobowski, 2015; Wooding and Ramirez, 2022). Numerous strategies have been explored to improve palatability such as the incorporation of sweeteners, bitter blockers, and cyclodextrins, yet no single approach fully addresses this adherence challenge (Walsh et al., 2014; Flammer et al., 2024; Schwiebert et al., 2021).

Hospital pharmacies have traditionally turned to custom compounding to address these challenges; however, compounding alone has not resolved issues of taste and dosing precision (Heitman et al., 2019); highlighting the need for innovative approaches. Given these limitations, three-dimensional (3D) printing technology offers a transformative, scalable solution, providing precise and personalized dosing capabilities, particularly valuable for paediatric care where adherence is critical (Binson et al., 2021; Juárez-Hernández and Carleton, 2022).

3D printing enables the precise preparation of pharmaceutical forms layer-by-layer, with specific applications in personalized medicine and drug delivery. The adaptability of 3D printing is especially promising in hospitals, where it facilitates the on-demand production of medications tailored to individual needs (Huanbutta et al., 2023; Annereau et al., 2021). This flexibility is crucial for children, who require doses that standard manufacturing methods cannot always provide, thereby enhancing treatment precision and therapeutic outcomes. Semi-solid extrusion (SSE) 3D printing that uses semi-solid pharmaceutical inks (pharma-inks) extruded through a nozzle offers unique advantages.

While SSE-based 3D printing offers significant advantages, such as precise dose personalization, modular drug release, and improved palatability, it also faces several limitations that must be addressed. A key drawback is the longer production time compared to compressed dosage forms, due to the layer-by-layer printing process and the additional drying phase required for water-based chewable tablets. However, gummies can be dried in a conventional oven outside a cleanroom, providing flexibility for hospital-based compounding where controlled environments may be limited. Another challenge is the relatively lower drug loading capacity compared to compressed tablets. Moreover, the extrusion-based nature of SSE can affect printing precision and layer adhesion, potentially resulting in minor variations in tablet dimensions. Lastly, while hydrophilic excipients improve drug solubility, they may increase bitterness, posing a challenge for taste masking—especially in paediatric settings. Despite these limitations, SSE remains a promising approach for personalized medicine in hospital environments (Wang et al., 2023; Seoane-Viaño et al., 2021; Cerveto et al., 2024; Rodríguez-Pombo et al., 2024).

SSE-based 3D printing has gained significant attention for paediatric applications, allowing for the precise fabrication of dosage forms personalized to each child's age, weight, and metabolic needs (Basit and Gaisford, 2018). Recent studies have demonstrated SSE's potential for individualizing doses and achieving modified-release profiles, particularly beneficial for children who may struggle with swallowing or frequent dosing requirements (Rodríguez-Pombo et al., 2024; Chatzitaki et al., 2022; Yi et al., 2023; Panraksa et al., 2022; Li et al., 2019). Additionally, SSE technology supports the combination of multiple active ingredients and even the integration of medications with nutritional components, which can address the unique dietary needs of certain patients (Carou-Senra et al., 2023).

This study aims to harness the flexibility of SSE-based 3D printing to develop novel SMX/TMP chewable formulations tailored for paediatric patients to improve adherence, to enhance palatability, and to ensure precise, customizable dosing with suitable stability. Additionally, the clinical implementation of this 3D printed formulations in the Department of Clinical Pharmacy in Gustave Roussy hospital was assessed according to French compounding regulations. The stability and printability of stored pharma-inks was evaluated. 3D printed formulations were benchmarked against the commercial medicine (BACTRIM®). This research aims to improve therapeutic outcomes for paediatric patients, showcasing the transformative potential of 3D printing in personalized medication production.

2. Materials & methods

2.1. Materials

Sulfamethoxazole, Trimethoprim, glacial acetic acid and hydrochloric acid 1 N were purchased from Sigma Aldrich (Sigma-Aldrich chemicals, USA). Maltitol syrup (LYCASIN® 80/55), mannitol (PEARLITOL® 50C), and pregelatinized starch (LYCATAB® PGS) were provided by Roquette (Roquette Frères, Lestrem, France). Gelatine (Emprove® Ph Eur; Bloom degree 110 [90–130]) and sucralose were obtained from Sigma (Sigma-Aldrich chemicals, Saint-Louis, USA), and the water for injection from B.Braun (Aqua B.Braun, Melsungen, Germany), peppermint and cooling aroma were obtained from IFF pharma (International Flavors and Fragrances, New-York, USA). 20-mL Injekt® syringes were supplied by B.Braun (Saint-Cloud, France), food colouring was purchased from Exberry (GNT International B.V, Mierlo, Netherlands). Water, acetonitrile (ACN), triethylamine (TRA) and methanol were HPLC grade and purchased from VWR chemicals (Radnor, Pennsylvania, USA).

2.2. Method for developing a 3D-Printed drug in the hospital setting

The development of a 3D-printed drug form in the hospital followed an established process (Fig. 1). The first step is to prepare pharma-inks to be loaded into the 3D printer and print test batches, then optimize these two stages before scaling up and validating the process for clinical use.

The use of two independent batches was intended as an initial step toward validating the process reliability under routine hospital production conditions. Mastery of this process requires an understanding of the factors that determine accurate, precise, and repeatable printing. For this purpose, the rheological characterization of the pharma-inks was carried out in the hospital, accompanied by physical characterization. Similarly, the final pharmaceutical form obtained was studied within the hospital to ensure that the set objectives were met.

2.3. Pharma-ink development and characterization

2.3.1. Hospital preparation of pharma-inks

As outlined in Fig. 1, three types of pharma-inks were developed to support both immediate clinical application and exploratory research.

The first pharma-ink, containing both active ingredients (SMX and TMP) in a single mixture, was designed to produce single-layer chewable tablets for clinical application. This approach emphasizes simplicity, reproducibility, and dosage consistency.

Additionally, two separate pharma-inks were formulated, each containing only one of the active ingredients, to be printed in layers to create bilayer chewable tablets. This bilayer approach, also shown in Fig. 1, explores the potential to reduce bitterness by physically separating the drugs. Although exploratory, it could lay the groundwork for future taste-masking strategies.

The final formulations for each ink are provided in Table 1.

The pharma-inks were prepared to yield syringes containing 15 mL of pharma-ink. Gelatine was heated to 45 °C in a beaker containing water and stirred magnetically for 20 min at 300 rpm. Subsequently, Trimethoprim, Sulfamethoxazole, pregelatinized starch, mannitol 50C, dye, sucralose, and flavourings were weighed and mixed. The mixture was ground using an automatic mixing machine, Topitec Touch® (WEPA Apothekenbedarf, Hillscheid, Germany). A suitable mixing jar was used for grinding, in which steel balls were added to facilitate particle size reduction. After 25 min of mixing at 400 rpm, a homogeneous powder blend was obtained.

Next, the powder blend was gradually added to a beaker containing maltitol syrup 80/55, which was stirred at 200 rpm using an overhead stirrer (Ika RW 20 digital with an anchor stirrer). Once the powders were

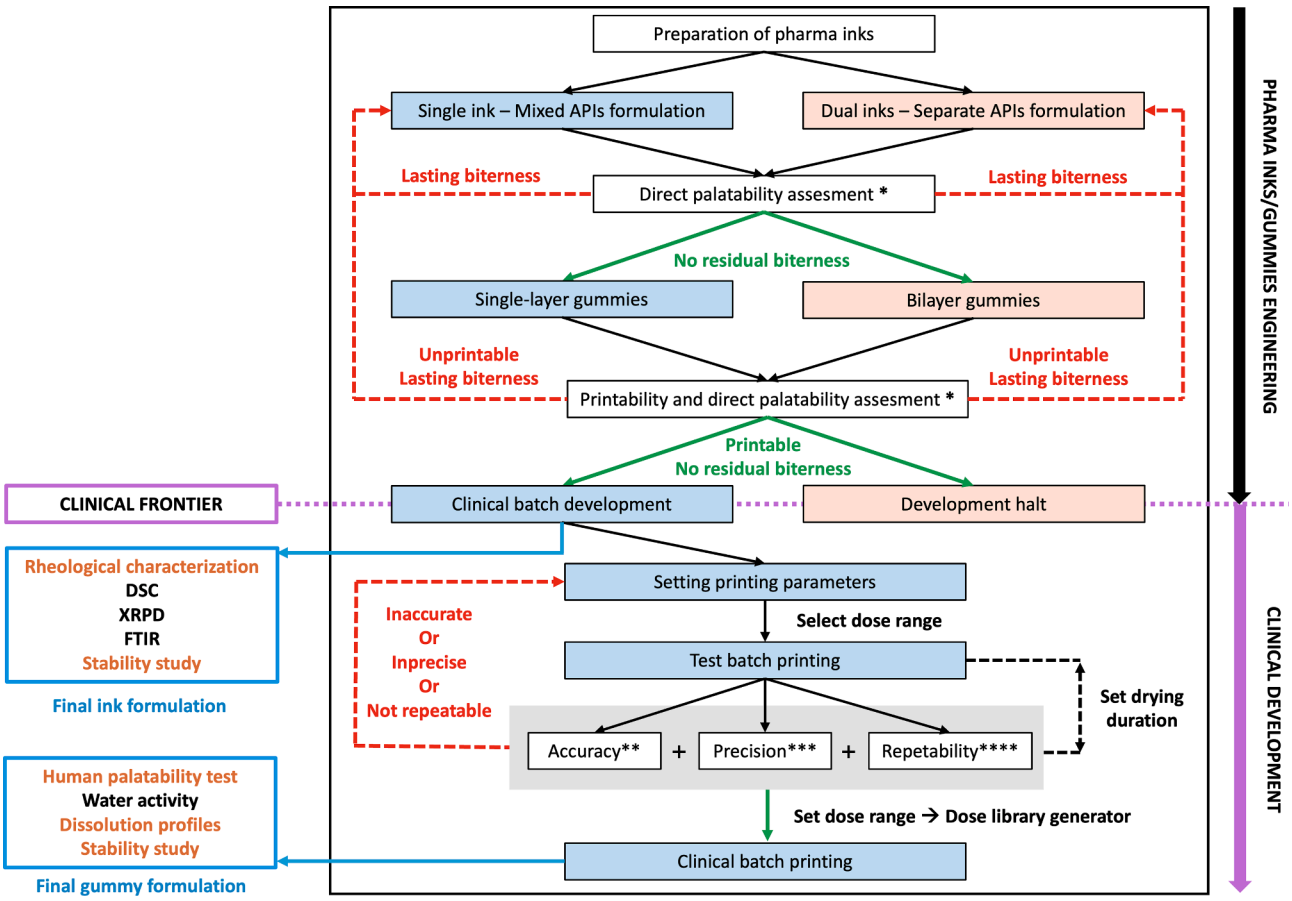

Fig. 1. Development Process Flow Chart for Clinical Batch Production in a Hospital Setting *Initial palatability assessment: Informal evaluation of bitterness by the formulator to exclude unacceptable formulations before printing. **Accuracy: The deviation of the average mass of printed chewable tablets from the theoretical target mass in each batch, aiming for less than 5%. ***Precision: Assessment of mass uniformity within each batch according to European Pharmacopeia, permitting a deviation of up to 5%. ****Repeatability: Validation of two independent test batches for accuracy and precision criteria for consistent dosing.

incorporated, the gelatine solution was transferred to the same beaker. After 2 min of additional mixing, the preparation was manually transferred into 20 mL B.Braun® syringes. The syringes were then cooled for 12 h at 2–8 °C, after which the pharma-inks were ready for use.

After preparation, the palatability of the pharma-inks was assessed by the formulator using the "swirl and spit" technique, with pharma-inks showing a bitter taste excluded from further stages.

2.3.2. *Pharma-ink rheological characterization*

The rheological properties of the hydrogels were studied using an MCR302 rheometer (Anton Paar, Austria) equipped with a Peltier hood HPTD 200 and a disposable aluminium measurement plate with a diameter of 70 mm, where the test samples were placed. An equilibration time of 10 min was set following sample deposition. The geometry used was a plate-plate measurement geometry with a diameter of 25 mm, and a gap of 1 mm was set for each measurement.

Amplitude sweeps were conducted by applying a strain ranging from 0.001 to 100 % at room temperature to evaluate the potential shear-thinning behaviour of the hydrogels. For this purpose, the storage modulus (G'), strain rate (γ), loss factor (tan δ) and limit of the linear viscoelastic region (LVE) were monitored for each sample. The linearity limit was calculated in terms of strain γ as a percentage, with a ± 5 % deviation (according to ISO 6721–10 standard) set as the tolerance range of deviation of G' around the plateau.

Subsequently, while maintaining a constant oscillatory shear within the Linear Viscoelastic (LVE) behaviour of the sample, the melting temperatures of the hydrogels were determined through temperature sweeps ranging from 25 to 90 °C, with a heating rate of 3 °C.min^{-1}. For this purpose, G' and tan δ were monitored for each sample.

Creep recovery tests were performed for a total of three cycles, in which a shear stress of 500 Pa was applied for 60 s – the approximate time required to obtain a chewable tablet of 1460 mg – followed by a subsequent time of 60 s without applying shear stress, during which the recovery of the analysed material was evaluated. Finally, tests were conducted to observe the ability of the ink present in the syringe to recover its properties after being heated to 45 °C. Briefly, after being heated to 45 °C for 20 min, the syringe was left at room temperature, and the storage modulus was observed immediately, as well as after 15 min, 30 min, 2 h, and 6 h of rest at room temperature during a heating step from 23 to 45 °C. Each measurement was performed without replicates, at the indicated time points. Data collection was performed using the RheoCompass software (version 1.32) of the instrument.

2.3.3. *Thermogravimetric analysis (TGA)*

TG measurements were performed with an STA 6000 thermogravimetric analyser (Perkin Elmer, Villepinte, France) equipped with a chiller water circulator and controlled by Pyris 13.3 software. Compounds or ink samples were placed in an open alumina crucible (200 µL) and loaded in the furnace. The initial weight of the samples was around 20 mg, and nitrogen was used as the purge gas at a constant flow of 20 mL.min^{-1}. The weight of the material was recorded during heating from 30 to 600 °C at a heating rate of 10 °C.min^{-1} after isotherm at 30 °C for 1 min. Each measurement was performed without replicates.

2.3.4. *Differential scanning calorimetry (DSC)*

High-speed differential scanning calorimetry (hyperDSC)

Table 1
Formulations of single and bilayer SMX/TMP pharma-inks. (%w/w): mass concentration in percent.

Materials	Pharma-ink composition for single layer tablets (%w/w)	Pharma-ink composition for bilayer tablets (%w/w)		Rational/Function
		SMX	TMP	
Water	12.0	12.0	12.0	Solvent and dispersing medium.
Maltitol syrup 80/55	40.5	40.0	52.0	Sweetener and texture.
Pregelatinized starch	7.2	7.3	8.3	Binder. Improves the integrity and chewability of the tablet.
Mannitol 50C	20.8	9.0	18.0	Osmotic filler. Reduced in the SMX layer to account for the large amount of SMX.
Gelatine	2.0	2.0	2.0	Gelling agent. 1/6 of the amount of water to improve the mechanical stability and printability of the ink.
Sucralose	0.5	1.2	1.2	Sweetener. Improves palatability. Increased quantity in the bilayer tablet to account for the high concentration of active ingredient.
Sulfamethoxazole (SMX)	13.7	27.4	–	Active ingredient.
Trimethoprim (TMP)	2.7	–	5.4	Active Ingredient.
Colouring	0.1	0.1	0.1	Aesthetic agent, improves visual appeal.
Aroma	0.5	1.0	1.0	Taste-masking agent, reduces bitterness perception. Increased quantity in the bilayer to account for the high API concentration.

experiments were carried out using a DSC8500 calorimeter (Perkin Elmer, Villepinte, France) equipped with an Intracooler II and controlled by Pyris 13.3 software. HyperDSC Aluminium Sample pans were filled with around 2 mg of the studied compound or ink with a balance sensitive to 0.01 mg and sealed. The compounds or ink samples were heated from −70 °C to a maximum of 280 °C at 700 °C.min^{-1} depending on the compound. Each measurement was performed without replicates. The objective was to observe the behaviour of the drugs within the final form before degradation began.

2.3.5. X-ray powder diffraction (XRPD)

The XRPD experiments were performed on both pharma-inks and samples on a Aeris Research Edition diffractometer (Malvern Panalytical, Palaiseau, France) with a sample changer of 6 positions and a PIXcel 1D detector. The working power is 300 W (30 kV − 10 mA). The used radiation is copper $K_{\alpha 1 + \alpha 2}$ (approx. 1.5406 Å). Compounds or ink samples were placed on a Si (510) zero background sample holder (AlpyX, Sainte-Hélène-du-Lac, France). Data were measured from 2 to 60° in 2θ with a total scan time of 10 min per scan and a rotation of the sample during acquisition. Each measurement was performed without replicates.

2.3.6. Infrared hyperspectral imaging (IHI)

IHI experiments were conducted using a PerkinElmer MIR/NIR Spotlight 400 Imager. Measures were performed on ink filament samples. The images obtained in the mid-IR using ATR imaging, ranging from 4000 cm^{-1} to 690 cm^{-1} with a spectral resolution of 8 cm^{-1} and a pixel size of 1.5 µm. The near-IR image in reflection mode ranges from 7800 cm^{-1} to 4000 cm^{-1}, with a resolution of 16 cm^{-1} and a pixel size of 25 µm. Each measurement was performed in duplicate. Both images are followed by a principal component analysis with 8 factors. The factors corresponding to SMX and TMP are displayed in red and green respectively.

2.4. Chewable tablet development and characterization

2.4.1. 3D printing setting

The 3D printing process, summarized in Fig. 1, was conducted using the M3DIMAKER 2 (FABRX, London, UK) pharmaceutical 3D printer. The printing parameters were established with an extrusion temperature of 40 °C, an 18G conical nozzle, a printhead movement speed of 20 mm/s (60 mm/s during non-printing), an infill density of 20 %, a first layer height of 1.6 mm, and subsequent layer heights of 1.2 mm. The tablets were printed onto a silicone and fiberglass plate to enhance adhesion. Notably, the printhead used a standard 20 mL syringe (B.Braun), facilitating easy material loading. All settings were managed using M3DIMAKER Studio software.

The tablets were printed onto a silicone and fiberglass plate and the printhead utilized a 20 mL syringe (B.Braun) to facilitate easy material loading. All printing settings were controlled through M3DIMAKER Studio software.

Single-layer printing was prioritized for clinical use, using three SSE print heads loaded with the same ink mixture to produce batches containing more chewable tablets. In contrast, bilayer printing was tested as a future-oriented application, with separate phama-inks in each print head for each drug.

After printing, the chewable tablets were dried for 24 h and the palatability was assessed by the formulator using the swirl and spit technique, with chewable tablets showing a bitter taste excluded from further stages.

2.4.2. Hospital clinical batch production

As illustrated in Fig. 1, the clinical batch development process involved producing test batches that met essential criteria: accuracy, precision, and repeatability.

The accuracy criterion required that the average tablet mass deviated by less than 5 %, and no unit differ more than 10 % from the theoretical target mass. This ensured that the dosage remained within acceptable limits and that the formulation provided reliable therapeutic dosing. Accuracy was calculated as shown in Eq. (1):

$$Accuracy\,(\%) = \frac{Average\ mass\ obtained - Theoretical\ mass}{Theoretical\ mass} \times 100 \qquad (1)$$

Precision was validated through mass uniformity testing, following the European Pharmacopoeia (Ph. Eur.) guidelines for tablets (EDQM, 2024). This process involved weighing each chewable tablet in the batch using an analytical balance (XPE 205 DeltaRange®, Mettler Toledo, Greifensee, Switzerland) to ensure compliance with mass uniformity standards. Specifically, for tablets with a weight of 250 mg or more, the Ph. Eur. permits a deviation of up to 5 % from the average mass. Any chewable tablets with individual weights falling outside the ±5 % range were considered non-compliant and were excluded from the batch. This process confirmed that the formulation met the required consistency, and that the dosage was uniformly distributed.

To ensure repeatability, two independent test batches were produced, each required to meet both the accuracy and precision criteria. Only when both batches passed these standards did the process advance to the dose library generator phase. This step established a reliable

correlation between the theoretical dose and the actual mass, thereby ensuring consistent dosing across all clinical batches.

In cases where any of these criteria were not met, adjustments were made to the printing parameters before a new test batch was produced. This systematic approach ensured that only formulations meeting stringent quality standards proceeded to clinical batch printing, thus reinforcing the reliability and reproducibility of the manufacturing process.

2.4.3. Preliminary palatability assessment

Palatability test were conducted on human adult volunteers using a sensory approach, to compare the newly developed SMX/TMP chewable tablets formulation with the only children's formulation available on the French market (BACTRIM® 40 mg/mL − 8 mg/mL oral suspension) (Clapham et al., 2023).

Two separated sensory evaluations were conducted to assess key palatability attributes through two questionnaires, one for each dosage form (Supplementary Table S1). 6 healthy volunteers participated in this unblinded, prospective, single-centre study using the swirl and spit method (N = 6). The evaluation employed the Swirl and Spit method to assess the palatability of both dosage forms. This method enabled the assessment of taste and aftertaste to ensure minimal systemic exposure to the product, thereby making it highly suitable for pharmaceutical sensory studies. During the evaluation, each participant received the newly developed chewable tablet and the marketed oral suspension in a randomized sequence. For the tablet evaluation, a pre-weighed chewable tablet was placed on the tongue and gently chewed for a period of 10 to 15 s before being swirled in the mouth to ensure uniform dissolution and optimal interaction with the taste receptors. In the case of the oral suspension, an equivalent dosage was administered to match the active pharmaceutical ingredient content present in the chewable tablet. After each evaluation, the participant was instructed to spit the sample into a designated container. A one-minute waiting period was observed before allowing the participant to rinse their mouth, as patients do not typically rinse immediately after administration of this type of pharmaceutical form. The study was carried out with at least one day between sessions to prevent any carryover effects from the sensory evaluation.

The study adhered to the Helsinki Declaration for biomedical research involving humans and followed Good Clinical Practice (GCP) guidelines.

Each volunteer was asked to complete the two questionnaires (one for the chewable tablet and one for the oral suspension). Each questionnaire assessed sweetness, texture, immediate bitterness, and lingering bitterness, as well as an overall acceptability score (global) using a 5-point Likert scale expect for sweetness, which uses a three-point scale, considering that sweetness can sometimes be perceived as excessive (Supplementary Table S1).

The main objective was to assess the impact of a change in dosage form on palatability. The primary outcome measured was the average score out of 23 points for each formulation. Secondary objectives included evaluating the impact of a change in dosage form on sweetness, immediate bitterness, and lingering bitterness. The secondary outcomes measured were the respective average scores for the associated sensory criteria.

Descriptive analysis of parameters was conducted on the intention-to-treat population. For all analyses, the statistical threshold (α) selected to consider a statistically significant difference was 0.05. To address both the primary and secondary objectives, paired samples comparing Wilcoxon rank-sum tests were performed, and the results were approximated using a rank-based analysis of variance through an ANOVA test. Results were expressed as medians.

2.4.4. Water activity (a_w)

A LabMaster-aw neo (Novasina, Neuheimstrasse, Switzerland) was used to measure the water activity of SMX/TMP chewable tablets. Briefly, prior to each measurement, a calibration curve was conducted according to the ISO18787 method, using 3 standards: 0.753, 0.843, and 0.973. Subsequently, measurements were taken on 3 randomly chosen chewable tablets that had been prepared beforehand and kept at room temperature (N = 3), with the water activity measured immediately after production and after 24 h of drying at room temperature.

2.4.5. In-vitro dissolution

In-vitro drug release profiles were obtained using a United-States Pharmacopeia (USP) Type II (paddle method) dissolution test apparatus, model Xtend 7, from Sotax (Saint-Louis, France). The dissolution tests employed the buffer specified in the USP monograph for Sulfamethoxazole/Trimethoprim tablets (USP, 2015). The method was designed to meet the specifications outlined in the European Pharmacopoeia monograph 2.9.3, which includes criteria for drug released over specified times (EDQM, 2024).

First, six randomly selected chewable tablets were weighed post-printing and dissolved in 900 mL of 0.1 N hydrochloric acid. The rotation speed was set to 75 rpm and the test duration fixed at 1 h. The content of each gummy was required to be ≥70 % of the theoretical content following USP monograph NF24.

2.4.6. Comparison of dissolution kinetics

The 3D printed tablets, the commercial oral suspension (BACTRIM® 40 mg/mL + 8 mg/mL, with one millilitre containing 40 mg of SMX and 8 mg of TMP, manufactured by Roche, Basel, Switzerland), and the commercial Sulfamethoxazole/Trimethoprim tablets (BACTRIM® 400/80 mg, containing 400 mg of SMX and 80 mg of TMP), were tested. An amount of each formulation containing 400/80 mg was used to obtain an accurate comparison. 12 samples of each speciality were analysed (N = 12). Each formulation was placed in 900 mL of 0.1 N hydrochloric acid at 37 °C with a paddle stirring at 75 rpm. Samples of 1 mL were withdrawn at specified intervals (0, 5, 15, 30, 45, and 60 min) and immediately replaced with fresh HCl to maintain constant volume. The drug release was quantified using the developed HPLC method. The dissolution kinetics were compared using the similarity factor f_2. The f_2 values were determined using **Eq. (2):**

$$f_2 = 50 \times \log\left\{\left[1 + \frac{1}{n}\sum_{t=1}^{n}(R_t - T_t)^2\right]^{-0,5} \times 100\right\} \quad (2)$$

Eq. (2): where n, R_t, and T_t represent the number of time and mean cumulative drug release of the reference and test profiles at each time point, respectively.

2.5. Analytical method and stability study

2.5.1. Drug quantitative determination

The quantitative determination of SMX/TMP were performed on a reversed-phase, high performance liquid chromatography (HPLC) component system LC 1260 (Agilent 1260 Series, Santa Clara, USA) consisting of an online degasser, quaternary pump, column heater, autosampler and UV/Vis detector and a column μBondapak C18 Column (Waters, Milford, USA), 125 Å, 10 μm, 3.9 × 300 mm. The method was developed according to Kulikov et al. (FDA, 2001). The mobile phase made of water/acetonitrile/triethylamine (799/200/1, *v/v*), buffered to pH 5.9, was set as the rate of 2 mL/min in isocratic mode. The column was thermoregulated at 30 °C. The injection volume was 50 μL. The detection wavelength was set at 254 nm. Standard stock solutions were Trimethoprim 388 mg/L and Sulfamethoxazole 169.9 mg/L in 100 % methanol. Working standard solutions were to obtain concentrations within the range of interest 17 to 153 μg/mL for SMX and 19.4 to 65.96 μg/mL for Trimethoprim. Analytical method validations were conducted according to ICH guidelines Q2(R2) and Q3B(R2) in order to evaluate specificity, linearity, repeatability, intermediate fidelity and limit of

detection (LOD) and limit of quantification (LOQ) (ICH, Q2(R2), 2023; ICH, Q3B(R2), 2006). Concerning the specificity evaluation, forced degradation studies were performed in accordance with ICH Q1A(R2) guidelines (ICH, Q1A(R2), 2003) (see section 2.5.2). A summary of the method validation parameters is available in Supplementary Table S2. Prior to any quantification, the samples were transferred into 500 µL microcentrifuge tubes. They were then centrifuged at 10,000 rpm for 10 min to prevent insoluble or poorly soluble excipients from polluting the HPLC system. Dilution with the mobile phase subsequently ensured a theoretical concentration within the validated concentration range.

2.5.2. Drug stability under stress conditions

Forced degradation studies of SMX and TMP were conducted under oxidative, hydrolytic, and thermal conditions using the previously validated method (2.5.1.). Hydrolytic degradation was evaluated in 0.1 N HCl and 0.1 N NaOH solutions at room temperature over 24 h. Oxidative stress testing was performed in solution using 0.3 % hydrogen peroxide with 1 $mg{\cdot}mL^{-1}$ of each drug, stored at room temperature and analysed at 0, 24, and 48 h. Thermal degradation was assessed by exposing solid-state API samples to 80 °C for 48 h.

2.5.3. Stability study

To determine the storage stability of the chewable tablets and hydrogels, a stability study was conducted in accordance with the ICH Q1A(R2) guidelines (ICH, Q1A(R2), 2003). The storage temperatures were either ambient (15–25 °C) or refrigerated (2–8 °C), and the samples were stored in various containers, including brown glass bottles, brown polyethylene terephthalate (PET) bottles, blister packs, or 20 mL B. Braun syringes. All SMX/TMP chewable tablets were stored away from light under conditions that allowed for potential oxidation. A total of 74 samples (72 chewable tablets and 2 syringes of the final formulation) were prepared from a single batch.

The physical stability of the chewable tablets and hydrogels was assessed by monitoring their organoleptic characteristics (odour, colour, mass), as well as the water content loss for the chewable tablets and the hydrogels in syringes (data not shown). For the pharma-inks, a study of their rheological properties over time was conducted to understand potential variations in physical properties that could occur during the printing process. To this end, amplitude sweeps were performed, and shear deformation was monitored according to section (2.3.2).

SMX and TMP were quantified by HPLC, and degradation products were analysed using the validated stability-indicative method. Physical and chemical stability tests were conducted at specific time points during the study (0, 15, 30, 90, and 180 days). A reduction in drug content greater than 5 % was established as the stability threshold. The evaluations were conducted in parallel on three chewable tablets (N = 3) or 3 pharma-inks (N = 3) test samples with a mass corresponding to 100/20 mg of SMX/TMP for the to minimize the risk of erroneous conclusions.

3. Results & Discussion

3.1. Pharma-ink development and characterization

3.1.1. Hospital preparation of pharma-inks

The formulation was designed to achieve optimal palatability, printability, and structural integrity. Excipient amounts were selected based on functionality and optimized through extensive trials (>80 iterations) to balance physical stability with effective taste masking, in particular to address the pronounced bitterness of TMP and SMX (Shinotsuka et al., 2023). Bilayer formulations were derived from the single-layer prototype with adjusted proportions to maintain performance while enabling API separation and improved taste masking. Several key ingredients played distinct functional roles in this formulation.

Maltitol syrup served as a sweetener, improving both taste and texture while also helping to reduce bitterness. In addition, it remains soft at around 30 °C, thus ensuring an optimal temperature range for printing (Rowe et al., 2009). Gelatine provided mechanical stability and a chewable texture; more importantly, by forming a three-dimensional network upon cooling, it trapped water and consequently limited the rapid hydration of pregelatinized starch, preventing excessive stickiness (Schrieber and Gareis, 2007; Andreazza et al., 2023). Pregelatinized starch itself acted as a binder, enhancing overall tablet integrity and chewability (Whistler and BeMiller, 2009). Mannitol is expected to facilitate drying and improve both the texture and drying behaviour of the final printed tablets due to its low hygroscopicity and osmotic properties, which may promote water migration, reduce overall moisture retention, and accelerate the drying process. These properties also contribute to a smoother mouthfeel suitable for paediatric patients (van Krevelen and te Nijenhuis, 2009). Finally, sucralose was selected for its intense sweetening properties, further enhancing palatability. Aroma and colouring agents were included to boost sensory appeal and support taste masking efforts (Alessandrini et al., 2023).

Together, these components ensured that the formulation met its objectives of being palatable, printable, and structurally sound.

3.1.2. Rheological characterizations

Characterizing the rheology of pharma-inks over time is crucial for understanding how their printing properties evolve. By correlating changes observed during printing with those from rheological measurements, optimal printing settings can be more effectively predicted.

The evolution of the storage modulus (G') and tan(δ) during a shear strain increase for ink at different time points, (Day 1, D8, D20, D33, D47) is shown in Fig. 2**A**. These data are essential in understanding the rheological behaviour of the ink over time, which directly impacts its printability and the quality of the final product.

The evolution of the storage modulus, representing the elastic component of the material's response to deformation, is presented in Fig. 2**A**. These data provide essential insights into the rheological behaviour of the ink over time, directly influencing its printability.

The decrease in the storage modulus (G') observed for the ink in response to increasing shear strain is typical of a polymer-based gel (Ferry, 1980). This behaviour may reflect the shear-thinning of the polymer chains and/or result from the disentanglement of polymer chains under stress (Wedamulla et al., 2023). These curves show a noticeable slope indicating ink softening beyond a shear strain of 1 %. The optimal printing zone lies along the initial part of this slope (before the crossover of G' and G''), corresponding in this study to values of $5{,}000 < G' < 12{,}000$ Pa.

The shift of the linear viscoelastic region (LVE) towards higher shear strain values over time reflects the evolution of the ink from D1 to D47. This increase in the storage modulus is likely due to the combined effect of continuous polymer crosslinking, possible water evaporation from syringes at ambient temperature, and gel syneresis (the expulsion of water from the gel) (van Krevelen and te Nijenhuis, 2009). These phenomena lead to gel stiffening and raise concerns about the ink's ability to remain printable.

Tan(δ), the ratio of the loss modulus (G") to the storage modulus (G'), provides insights into the material's damping properties, i.e., its ability to dissipate energy. Here, tan(δ) values remain relatively constant over time. This indicates that, despite the stiffening of the ink over time, the balance between the elastic (solid-like) and viscous (liquid-like) behaviour of the ink remains stable. This stability is crucial for predicting potential physical instability as the ink ages, although it is insufficient alone to predict the ink's printability.

For the developed formulation, extrusion required a minimum applied force of 20 Newtons (N), and the extrusion flow became stable at around 40 N, corresponding to a pressure of 1.27×10^5 Pa with an 18G conical nozzle. Monitoring these values could help predict printability and adjust the printing parameters based on observed fluctuations, for example, by correlating the necessary increase in printing temperature

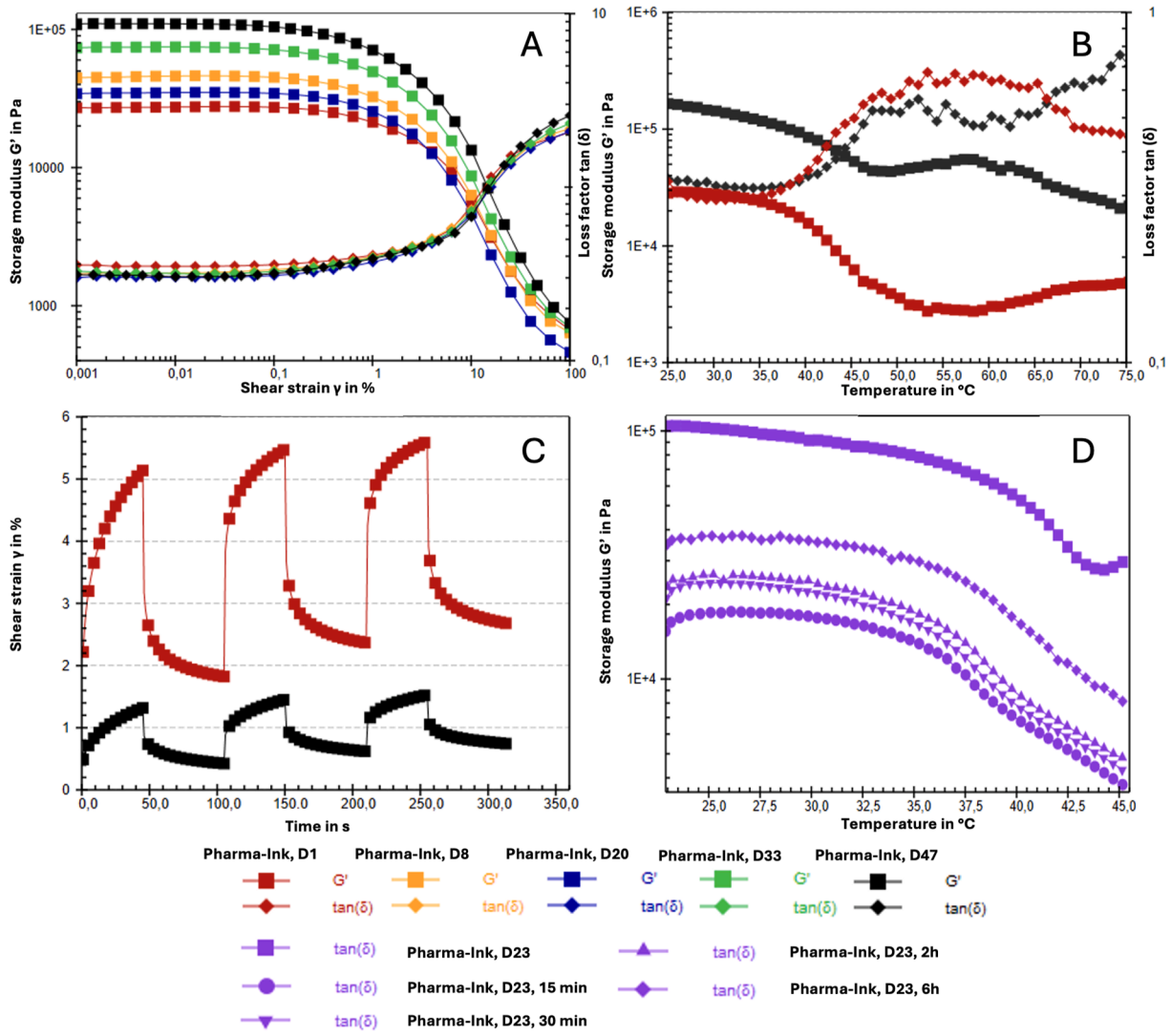

Fig. 2. Rheological Characterization of pharma-inks for 3D Printing Applications. Fig. 2**A**: Evolution of storage modulus (G') and tan(δ) during shear strain increase for ink at different time points (D1, D8, D20, D33, D47). Fig. 2**B**: Comparison of storage modulus (G') and tan(δ) during a temperature ramp from 25 to 75 °C for ink at D1 and D47. Fig. 2**C**: Shear stress behaviour over time under constant shear strain for ink after 47 days of storage at room temperature. Fig. 2**D**: Storage modulus (G') during temperature ramp from 23 to 45 °C for ink at D23 depending on rest time of the ink after heating for 20 min at 45 °C. Each measurement was performed without replicates, at the indicated time points.

with the increase in G' over time.

Determining optimal printing temperatures is another key benefit of rheological analysis. The inflection points of tan(δ) and G', presented in Fig. 2**B**, correspond to the gel softening temperatures and, therefore, to the optimal printing temperatures. For the ink at D1, the optimal printing temperature range is between 35 and 40 °C, consistent with the values already discussed in Fig. 2**A**. Within this range, the gel flows without becoming too liquid, allowing for precise layer-by-layer deposition.

The thermal behaviour of the ink is typical of crosslinked polymers, which soften without melting, even at temperatures well above the defined printing temperature. This property is crucial for maintaining print fidelity and is consistent with studies showing that the quality of 3D printing depends on the ink's flow behaviour, viscosity, and thermal properties (Azad et al., 2020; Wedamulla et al., 2023; Chen et al., 2019).

After 47 days of storage at room temperature, the gel becomes harder, as illustrated in Fig. 2B and C, rendering it unprintable. This increase in hardness is consistent with possible water loss during storage and aligns with research on gelatine crosslinking and its impact on gel hardness (M'Barki et al., 2017; Djagny et al., 2001). At D47, G' exceeds 12,000 Pa for temperatures below 65 °C, explaining the ink's unprintability at this point.

The thixotropic nature of the ink was confirmed through recovery tests, which show that after the removal of shear stress, the ink partially recovers its structure (Fig. 2**C**). These results confirm the reversibility of crosslinking within the polymer matrix of our ink and are consistent with the findings of Modigell et al. (Modigell et al., 2018), who demonstrated that recovery depends on the storage duration (which causes initial deformation) and the resting time of the analysed material. This underscores the importance of defining resting times between successive uses of the same syringe and highlights the relevance of this type of test in the development of semi-solid formulations for 3D printing (Junnila et al., 2024).

In clinical applications, the goal is to produce chewable tablets on demand. Depending on the required dosage, syringes may be heated and then returned to storage. To better determine the resting time necessary for restoring the ink's rheological properties after heating, temperature ramp tests were performed on the ink after different resting periods (Fig. 2**D**). The results indicate that a resting period of 6 h is insufficient for the ink to recover its initial rheological properties. In practice, a

resting period of 24 h should be observed before reheating a syringe to ensure printing precision and consistency.

These results demonstrate that rheological and thermal properties are essential for ensuring the quality of 3D-printed dosage forms. The storage modulus (G') and tan(δ) can serve as key indicators of printability, ensuring consistent flow and structural stability of the printed layers. As noted by Suárez-González et al. (Suárez-González et al., 2024), monitoring these properties over time could enable adjustments in printing parameters to maintain optimal formulation quality. Although real-time pressure measurements during extrusion may be more straightforward and practical for routine use (Junnila et al., 2024; Díaz-Torres et al., 2022), the integration of the methodology used in this study could help optimize printing parameters and ensure the production of consistent and reliable 3D-printed medicines throughout their shelf life.

3.1.3. *Thermal and structural characterizations*

Thermal and structural characterizations are essential for understanding the behaviour of each component in gummy formulations, particularly in terms of their stability and performance during

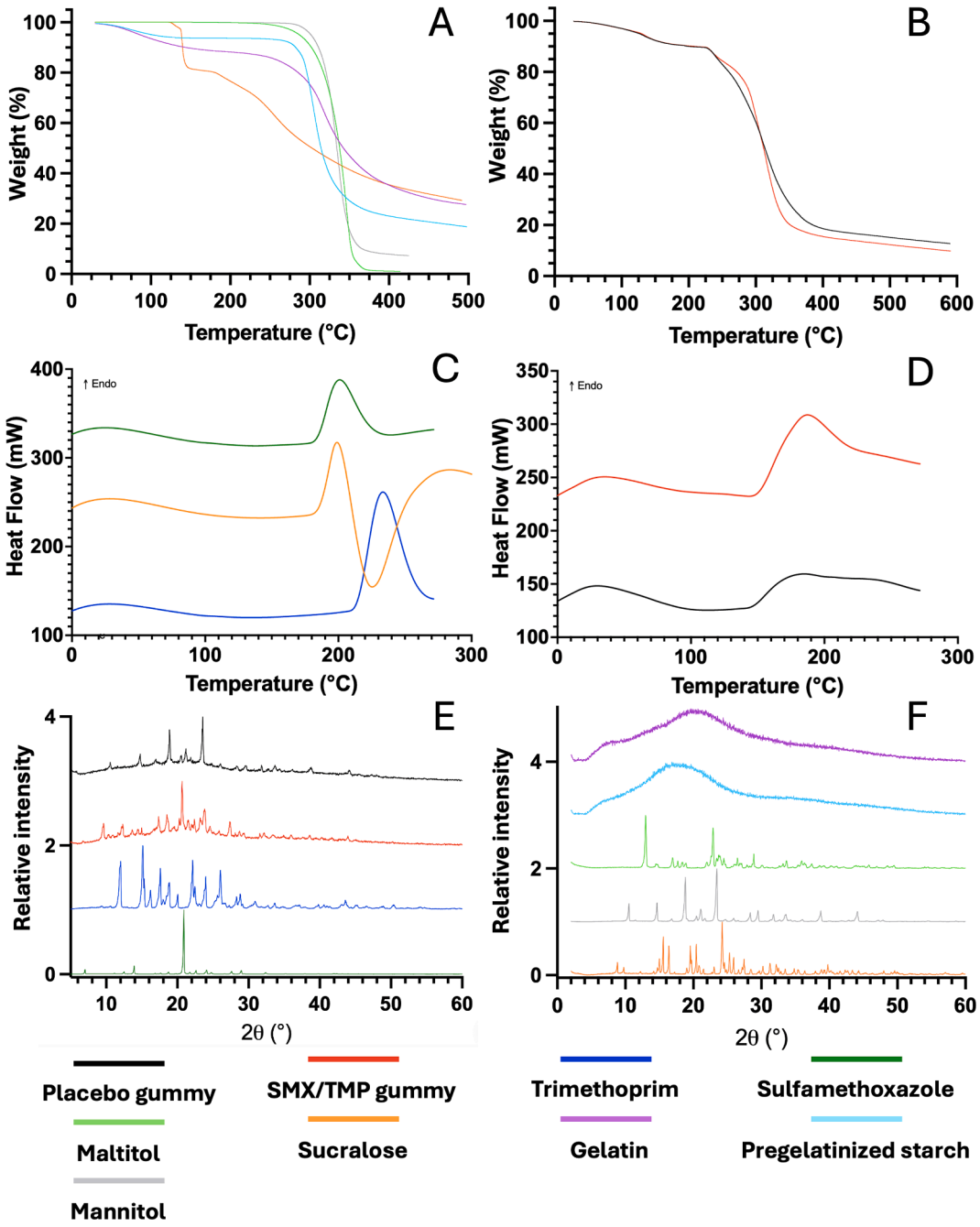

Fig. 3. Characterization of gummy formulations and individual components. Fig. 3**A.** Thermogravimetric analysis (TGA) curves, obtained at a heating rate of 10 °C.min^{-1}, of individual excipients, showing weight percentage (%) versus temperature (°C). Fig. 3**B.** TGA curves, obtained at a heating rate of 10 °C.min^{-1}, comparing the mass loss of filament and placebo filament, showing weight percentage (%) versus temperature (°C). Fig. 3**C.** High-speed Differential Scanning Calorimetry (DSC) heating curves, obtained at a heating rate of 700 °C.min^{-1}, showing heat flow (mW) versus temperature (°C) for individual components. Fig. 3**D.** High-speed DSC heating curves, obtained at a heating rate of 700 °C.min^{-1}, showing heat flow (mW) versus temperature (°C). Fig. 3**E.** X-ray powder diffraction (XRPD) patterns showing relative intensity versus 2θ (°) for gummy, placebo gummy, Sulfamethoxazole and trimethoprim. Fig. 3**F.** XRPD patterns showing relative intensity versus 2θ (°) for individual excipients. Each measurement was performed without replicates.

processing and storage. By analysing the thermal decomposition, crystalline structure, and interaction between excipients and active ingredients, it is possible to optimize the formulation to ensure product integrity, printability, and overall quality of the 3D-printed chewable tablets.

The evolution of the TGA curves, showing the weight percentage (%) versus temperature (°C) for individual components, is illustrated in Fig. 3**A**.

This analysis provides valuable insights into the thermal stability and decomposition behaviour of the excipients. Maltitol begins to decompose significantly around 300 °C, indicating its thermal decomposition. Sucralose exhibits a two-step decomposition process, with initial weight loss around 120 °C and gradual decomposition up to 500 °C, indicating relatively lower thermal stability compared to other components. This decomposition at 120 °C must be considered in the practical execution of DSC analyses. Mannitol remains stable up to approximately 300 °C, after which it undergoes pronounced weight loss. Gelatine starts losing weight around 100 °C, with gradual decomposition continuing up to approximately 350 °C. Pregelatinized starch shows gradual thermal decomposition starting around 250 °C, indicating moderate thermal stability. These thermal properties are crucial for determining the appropriate processing temperatures during gummy formulation and storage, ensuring that each component maintains its integrity during manufacturing.

The comparison of mass loss between the filament and a placebo filament as a function of temperature is shown in Fig. 3**B**. Both formulations initially lose mass due to water evaporation, followed by a rapid degradation phase starting at 225 °C. The filament shows a slight shift towards higher temperatures compared to the placebo, indicating that drug-drug or drug-matrix interactions enhance its thermal stability. This increased stability suggests that the presence of APIs strengthens the gummy formulation, improving its robustness during processing and storage.

The high-speed DSC heating curves, showing heat flow (mW) versus temperature (°C) for the individual components, are presented in Fig. 3**C**. Sulfamethoxazole (SMX) exhibits an endothermic peak at 169 °C, corresponding to its melting point, while Trimethoprim (TMP) shows an endothermic peak at 200 °C. These thermal events align with the literature (Agafonova et al., 2013; de Moura Oliveira et al., 2019; Fernandes et al., 1999) and confirm the crystalline nature of the APIs, providing essential baseline data for understanding their behaviour within the gummy formulations.

The high-speed DSC curves of the filament and the placebo filament reveal distinct thermal events starting around 120 °C, which may be associated with the melting of some excipients, such as mannitol and maltitol (Fig. 3**D**). A more pronounced endotherm is observed in the filament containing SMX and TMP, indicating that the drugs significantly contribute to the thermal transitions within the formulation. These characterization studies also revealed a glass transition between 60 and 100 °C within the active ingredient-loaded filaments, which was not observed with the placebo filaments (data not shown). The presence of a single glass transition temperature, as noted in the work of Li et ***al.*** (Li et al., 2022), could indicate that the drugs are present in a unified phase. However, it is also possible that they exist in both crystalline and amorphous forms within the formulation, affecting the physical stability, shelf life, and availability of the final product. These endothermic events provide key insights into the printing process, ensuring that the formulation remains stable during storage and use.

The XRPD patterns of the gummy and the placebo gummy, showing the relative intensity versus 2θ (°), are shown in Fig. 3**E.** The sharp peaks observed indicate that most of the components in the gummy formulations are crystalline. This high crystallinity, approximately 90 %, could contribute to the "sandy" texture of the 3D-printed chewable tablets, affecting their palatability. The peak observed at 21° (2θ) is characteristic of Sulfamethoxazole (SMX), while multiple peaks between 10° and 30° (2θ) indicate the presence of Trimethoprim (TMP). The analysis confirms that the chewable tablets consist of a dispersion of crystalline solids within an amorphous polymeric matrix, consistent with the properties of gelatine and pregelatinized starch used in the formulation. These findings align with the literature, as noted by previous studies (Alsubaie et al., 2018), confirming the structural nature of the components.

An analysis of the XRPD patterns of the individual excipients used in the gummy formulations reveals the crystalline and amorphous nature of the components (Fig. 3**F**). The two polymers, gelatine and pregelatinized starch, are amorphous, whereas the other excipients are crystalline. This pattern reinforces the earlier observation that high crystallinity in the components significantly influences the overall texture of the gummy formulations. The crystalline structure is a key factor contributing to the "sandy" texture often observed in the chewable tablets, which can affect their palatability. Understanding the crystalline structure of each component is essential for predicting how these excipients will interact in the final product. The degree of crystallinity in each excipient not only affects the texture but also plays a crucial role in determining the mechanical stability of the chewable tablets.

The XRD analysis confirms the crystalline nature of most components, which influences the texture of the chewable tablets. TGA and DSC analyses provide critical insights into the thermal behaviour of the formulations, highlighting their stability and potential processing challenges. These characterizations are essential for optimizing the formulation, ensuring its stability, and understanding how each component contributes to the overall performance of the 3D-printed chewable tablets.

3.1.4. Infrared hyperspectral imaging (IHI)

FTIR is a powerful tool for characterizing the spatial distribution of active ingredients and excipients within pharmaceutical formulations (Algahtani et al., 2021; Le et al., 2022). Similarly, infrared technology can be used to obtain images within formulations. By mapping the distribution of components, IHI provides critical insights into the uniformity, potential interactions, and stability of the formulation, all of which are key factors in optimizing the performance and palatability of 3D-printed pharmaceuticals (Khorasani et al., 2016; Kilpeläinen et al., 2022; van Haaren et al., 2023).

Fig. 4 focuses on the analysis of the distribution of active pharmaceutical ingredients (APIs) within the formulation using IHI. This figure provides detailed insights into the spatial distribution and potential interactions between the APIs within the gummy matrix, which are critical for understanding the formulation's palatability, stability, and overall performance.

The optical microscopy image of the formulation filament, as shown in Fig. 4**A**, highlights the area of interest for the infrared study, which is outlined in red. This area represents the specific segment of the filament analysed using IHI to assess the distribution of the APIs within the matrix. The visual representation provided by this optical image serves as a contextual reference for the subsequent IHI analysis, allowing for a clear understanding of the specific location within the filament from which the infrared data was collected. The uniformity or heterogeneity observed in this optical image offers preliminary clues about the distribution of the APIs, which is further detailed in the following IHI images. The size of the observed particles is comparable to that of the active ingredient particles: Sulfamethoxazole ranges from 150 to 200 μm, and Trimethoprim from 140 and 180 μm (based on internal supplier data).

The NIR image corresponding to the optical microscopy view highlights the distribution of SMX in red and TMP in green within the formulation filament **(**Fig. 4**B).** This color-coded image facilitates a clear distinction between the two APIs and their spatial arrangement within the filament. SMX appears to be more homogeneously distributed across the filament, indicating good dispersion within the matrix. Conversely, TMP tends to form clusters or agglomerates, indicating a less uniform

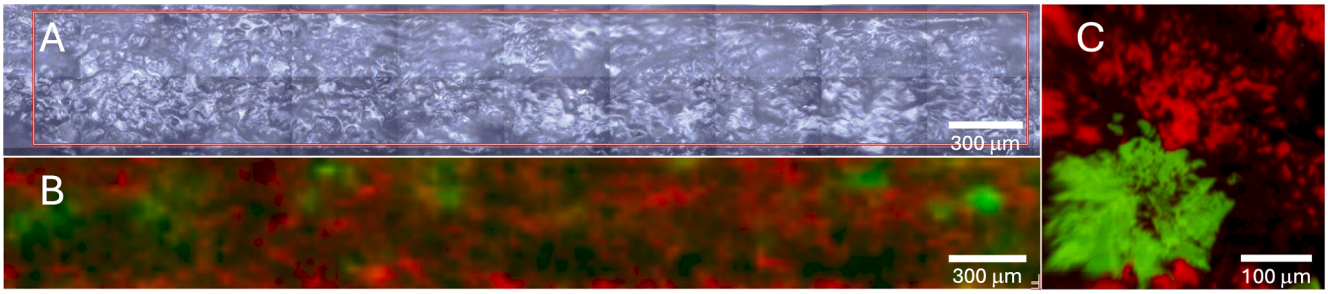

Fig. 4. Infrared hyperspectral imaging (IHI) Analysis of Formulation Filament. Fig. 4**A** Optical microscopy image of the infrared study area outlined in red, depicting the segment of the filament analysed. Fig. 4**B** Near-infrared (NIR) image corresponding to the optical microscopy view, highlighting the distribution of Sulfamethoxazole (SMX) in red and Trimethoprim (TMP) in green. Fig. 4**C** Vertical cross-section of the filament showing the distribution of the two active pharmaceutical ingredients (APIs) in Mid-infrared (MIR). Each measurement was performed in duplicate.

distribution. This clustering can be problematic as it may contribute to the bitter taste of the gummy, with TMP being primarily responsible for the bitterness. The distinct distribution patterns of SMX and TMP could also suggest potential interactions or co-localization within the matrix, which might influence the physical properties, such as dissolution behaviour, and the overall taste profile of the gummy.

A vertical cross-section of the filament in MIR, presented in Fig. 4**C**, further illustrates the distribution of SMX and TMP using the same colour coding, with red for SMX and green for TMP. This cross-sectional view provides a three-dimensional perspective, showing how the APIs are distributed not only across the surface but also throughout the depth of the filament. The cross-sectional view reaffirms the observations from the NIR image, with TMP showing a tendency to concentrate in certain regions, forming more significant agglomerates compared to SMX. The homogeneous distribution of SMX suggests that it is well-integrated into the matrix, which is beneficial for ensuring consistent dosage and potentially reducing the perception of bitterness. In contrast, TMP's tendency to cluster might contribute to variations in taste and could affect the uniformity of the dosage if not adequately controlled. This clustering might also influence the mechanical properties of the gummy, such as its texture and firmness, by creating regions with different consistency.

In summary, SMX is more evenly distributed within the matrix, contributing to consistent dosage and potentially better taste masking. TMP, however, shows a tendency to cluster, which could lead to localized bitterness and affect the overall sensory experience of the gummy. This clustering might also impact the mechanical properties and uniformity of the gummy, emphasizing the need for careful control of the formulation process to ensure a balanced distribution of both APIs. The insights gained from this IHI analysis are crucial for optimizing the formulation to enhance palatability, ensure consistent dosage, and maintain the mechanical integrity of the 3D-printed chewable tablets.

3.2. Chewable tablet development and characterization

3.2.1. 3D printing in hospital setting

In the development of chewable tablets for children, many printing parameters proved to be crucial. The size, first and foremost, is largely related to the concentration of active ingredients in the ink and the dose required for each patient. The advantage of 3D printing in this regard lies in its ability to print chewable tablets of various sizes and shapes, thus overcoming the limitation of using ink with a fixed concentration of active ingredients. This flexibility allows tailoring the formulation to individual patient needs, particularly important in paediatric settings where dosing often varies.

With this in mind, it was ensured that the print settings allowed for the repeatable production of monolayer tablets with active ingredient concentrations ranging from 100/20 mg to 400/80 mg of SMX/TMP. These concentrations correspond to tablets weighing between 730 mg and 2920 mg (Supplementary Table S3). The printing process resulted in accurate doses, with intra-batch mass variation averaging 2 % (Supplementary Table S4). This low variation demonstrates a reliable and reproducible printing process, essential for clinical use. Regarding printing accuracy, only the first gummy from each batch did not meet the dose uniformity requirement and had a mass more than 5 % below the theoretical mass. As a result, it was decided to systematically discard the first tablet printed from each syringe, ensuring that the rest of the batch met dosage standards.

Another critical aspect for clinical application is printing speed. With this aim, this work validated a configuration using three print heads with SSE technology Fig. 5**A**.

As shown in the simulation in Fig. 5**B**, each head was programmed to print 22 monolayer chewable tablets, which ultimately enabled the production of clinical batches of up to 66 chewable tablets, with a production rate of one 730 mg tablet every 24 s. For higher-dose formulations, the largest chewable tablet produced (weighing 2920 mg) required approximately 71 s to print under hospital production conditions **(Table S3)**. This high throughput demonstrates that the technology is scalable and can meet clinical demands efficiently.

Swallowability of oral dosage forms in children is a multifactorial consideration (Ternik et al., 2018). Although no official size has been defined as ideal for the paediatric population (EMA, 2013), this study aimed to limit the size of chewable tablets to improve compliance. The chewable tablets were designed to be chewed and then swallowed, making them particularly suitable for children who can chew (Fig. 6**A**). Based on current literature on children's preferences regarding oral dosage forms (Mistry and Batchelor, 2017; Saito et al., 2018), chewable tablets containing 100/20 mg of active ingredients would be ideal, even if it requires taking multiple tablets. As shown in Fig. 6**A**, this work successfully produced 730 mg single-layer chewable tablets by concentrating the active ingredients without compromising printability.

Following the printing process, the water content of the chewable tablets became a critical factor influencing their physical properties. Over a 24-hour drying period, the chewable tablets experienced about 14 % reduction in total mass. This mass loss corresponds to approximately 75 % of the initial water content, reducing the final water content to $\simeq$ 3–4 % (w/w) post-drying. Final values are compatible with the TGA profiles of the gummies observed. This controlled drying process was necessary to achieve the desired gummy texture while ensuring product stability.

Considering that the bitterness of the SMX/TMP combination comes from TMP, multi-head technology was tested to print the two layers of active ingredients separately. As shown in Fig. 6**B**, the size of the multilayer tablets was similar to that of the single-layer ones. Maintaining a manageable size for paediatric patients remains key, even when transitioning to bilayer formulations. For practical reasons, two different colours were used to easily distinguish the pharma-inks containing TMP or SMX. The bilayer tablet consists of two layers of equal height in these experimental gummies. The TMP (green) layer is deposited first, followed by the SMX (blue) layer on top. This ensures

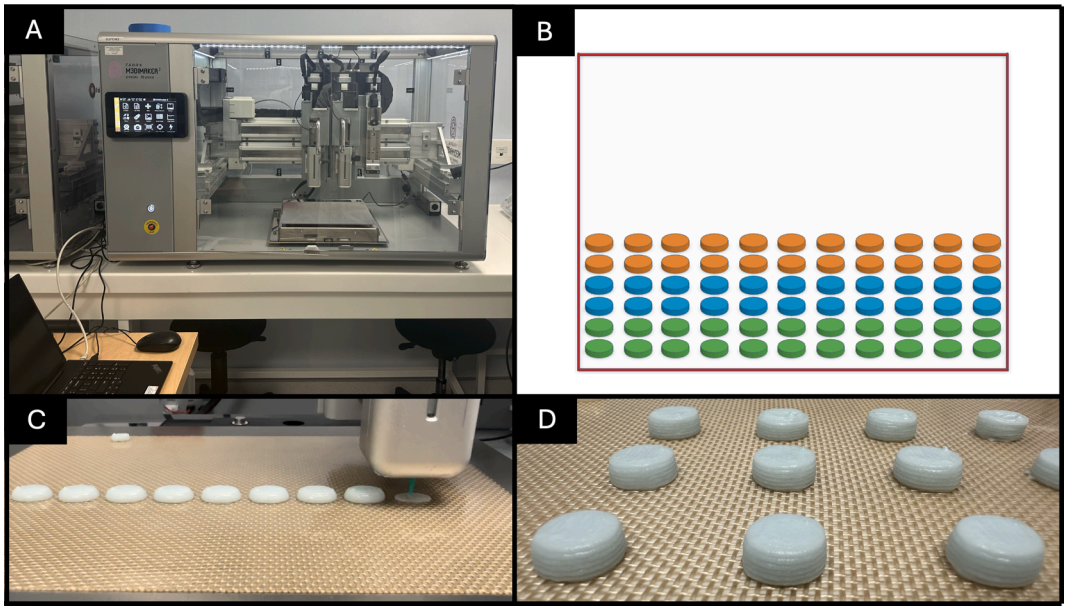

Fig. 5. Production of clinical batches of 3D-printed chewable tablets in a hospital setting. Fig. 5A. 3D printer equipped with two print heads for SSE technology printing. Fig. 5B. Computer simulation of clinical batch printing using three SSE print heads. Fig. 5C. SSE print head in operation during clinical batch production. Fig. 5D. Example of a printed batch.

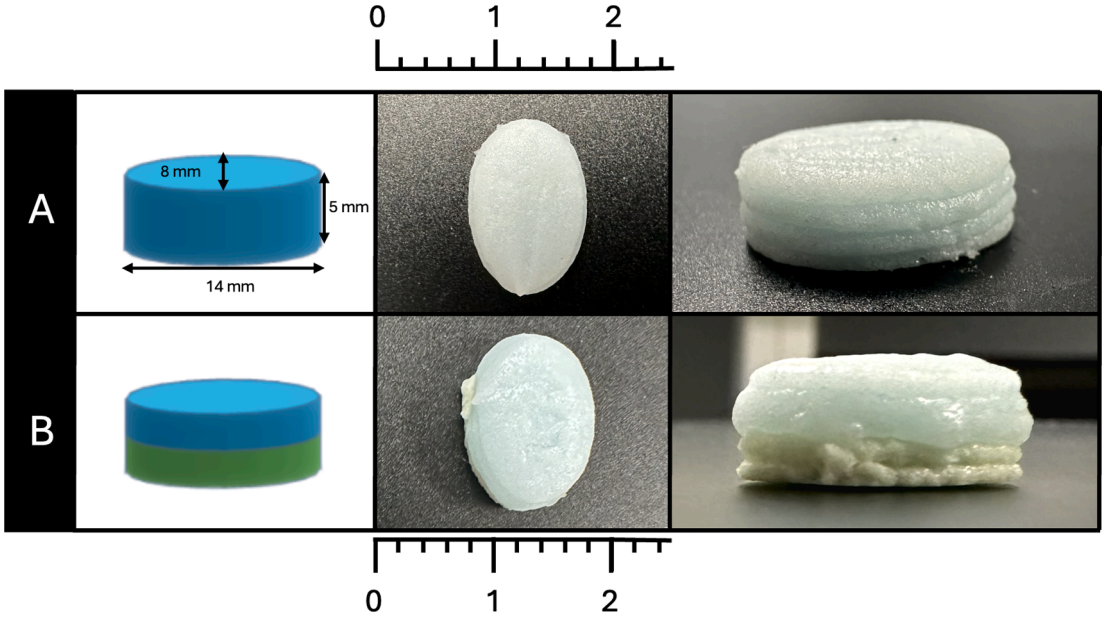

Fig. 6. Representation of monolayer and bilayer chewable tablets through simulation, top view (with the associated scale in cm), and side view. Fig. 6**A.** SMX/TMP (100/20 mg) monolayer gummy representations. Fig. 6**B.** SMX (blue)/TMP (green) (200/40 mg) bilayer gummy representations.

uniformity in layer distribution and facilitates the intended formulation design**.** Although a test batch of bilayer tablets was successfully printed, the technology does not currently allow for scaling up to clinical batch sizes, nor does it validate a robust printing process (Supplementary Table S5). Therefore, bilayer technology remains an innovative yet experimental solution, requiring future optimizations to achieve clinical scalability.

In previous single-layer formulations, a cola-flavoured ink was used, but it proved ineffective in adequately masking the bitterness of TMP. However, when this cola flavour was applied to bilayer chewable tablets, it eliminated the bitterness. This improvement is likely due to a greater dilution of TMP within its ink, increased use of sweeteners, and the absence of co-localization of the two APIs in the bilayer configuration. This significant enhancement in taste masking shows that the bilayer approach could be pivotal in improving patient adherence.

Given the success of the bilayer chewable tablets in improving palatability, future research could explore automating the bilayer production process. The development of dual-head printing systems for hospital use, as depicted in Fig. 5**A**, could streamline bilayer gummy production, minimizing manual intervention and optimizing workflow for routine use. This approach holds significant potential for scaling personalized medicine, particularly for paediatric patients who require frequent adjustments in dosage based on body weight and health conditions.

By developing efficient methods for printing personalized medications on demand, this research demonstrates the potential for 3D

printing technology to revolutionize pharmaceutical care, particularly in paediatric settings where the need for custom doses is critical. While monolayer chewable tablets have already shown promise, bilayer technology opens new avenues for improving taste masking and treatment personalization.

3.2.2. Preliminary palatability assessment

The palatability of a pharmaceutical formulation refers to how pleasant it is in terms of taste, smell, and overall sensory experience when given to patients. Oral formulations are often unpalatable, which is a major reason for children's non-adherence, especially with antibiotics (Baguley et al., 2012; Kardas et al., 2021; Soares et al., 2022). An unpalatable formulation can significantly reduce a young patient's willingness to take their medication, thereby reducing the therapy's effectiveness (Piana et al., 2017; Santer et al., 2014).

For SMX/TMP formulations, the best comparator is the BACTRIM® oral suspension. Our sensory study focused on four aspects of the palatability of the SMX/TMP gummy formulation compared to the suspension. The sensory evaluation results, presented in Table 2, utilized F-values and p-values derived from a rank-based analysis to assess the differences between the gummy formulation and the BACTRIM® oral suspension. In this study, a p-value of less than 0.05 ($p < 0.05$) was considered to indicate a statistically significant difference between the formulations. Evaluated attributes included texture, sweetness, immediate and lasting bitterness, and an overall "global" acceptability score reflecting the participant's general impression of the formulation. Each of the 6 volunteers evaluated both formulations, resulting in 12 observations per sensory attribute.

The analysis revealed that the suspension's texture was perceived as better than that of the chewable tablets ($F_{1,10} = 20.00$, $p < 0.01$), primarily due to the gritty texture of the chewable tablets, which is attributed to the crystalline nature of 90 % of the components in our polymeric dispersion. However, the results also indicate that persistent bitterness is significantly reduced by the gummy formulation ($F_{1,10} = 13.89$, $p < 0.01$), without a corresponding increase in perceived sweetness ($F_{1,10} = 0.38$, $p = 0.55$). This suggests that while the texture could be improved, the formulation effectively addresses bitterness, which is a critical factor for patient adherence. Additionally, the gummy formulation is generally preferred over the current oral suspension formulation ($F_{1,10} = 90.00$, $p < 0.01$), indicating a favourable overall sensory experience despite the texture issues.

To mitigate an unpleasant texture, modifications could be made. For example, a metal ball mixing process can finely grind the powders (de Oliveira Barros et al., 2023); However, this technique can lead to the particle size reduction of excipients and APIs in the formulation (Podgorbunskikh et al., 2022; Wang et al., 2023), with a possible modification of bitterness either through co-amorphization or co-crystallization (Li et al., 2022). In this study, this technique was employed to reduce the gritty texture of our formulation, and it was observed that this adjustment did not significantly impact the bitterness. Alternatively, polymers could be used to further disperse the APIs, but the tendency of our two APIs to co-localize within the matrix rendered this dispersion ineffective in a single-layer tablet.

In the context of optimizing palatability, sweetness and bitterness are closely linked. Indeed, some sweeteners like saccharin are known to leave a bitter aftertaste (Rowe et al., 2009). The SMX/TMP combination is particularly challenging due to its persistent bitter taste. Previous studies in rat models and electronic tongue models have shown that this bitterness is primarily due to TMP (Kojima et al., 2021); and that sucralose at a specific range can reduce bitterness (Shinotsuka et al., 2023). Nevertheless, the quantities of sucralose needed for optimizing sweetness in humans appear to be higher than those required for rats.

Many taste-masking strategies exist. The use of flavours, sweeteners, amorphization, ion exchange resins, cyclodextrins, and encapsulation techniques are widely described examples (Douroumis, 2007). However, a single method may not be sufficient to create a palatable product. Therefore, a combination of approaches may be necessary, especially for drugs with a strongly bitter taste. For example, in the case of TMP, even a very small amount of the active ingredient can significantly affect palatability.

While the data suggest a general preference for the gummy formulation, real life data will confirm that trend.

3.2.3. Water activity

Water activity (a_w) measures the availability of free water in a product to support biological and chemical reactions, influencing the product's stability, quality, and shelf life. The impact of a_w on microbial death, survival, sporulation, and toxin production has been extensively studied and is recognized as a critical control point in food product risk analysis (Gutiérrez-López et al., 2015).

In pharmaceutical preparations, the risk assessment of non-sterile products must include microbiological controls. The relevant monographs in the European Pharmacopoeia are Chapters 5.1.4 and 2.6.12 (EDQM, 2024). Although a_w measurement is covered by a European Pharmacopoeia monograph, it is not utilized by hospital pharmacies to ensure the microbiological safety of preparation (Sandle, 2016).

In the case of SMX/TMP chewable tablets, the use of these monographs seemed inadequate as they required the neutralization or removal of active ingredients with intrinsic antimicrobial effects. Therefore, a_w was used to determine the appropriate drying time to achieve a water activity level that ensures the absence of microbial growth and, by extension, provides a presumption of microbiological stability.

The a_w measured at 0 and 24 h were 0.836 ± 0.004 and 0.585 ± 0.004, respectively (N = 3). It is acknowledged that for a_w values below 0.6, microbial growth is impossible (Gutiérrez-López et al., 2015). These values allow us to quantify the microbiological risk and support the decision to package the chewable tablets after 24 h of drying in a controlled atmosphere area. Nevertheless, it is important to note that low a_w inhibits growth but does not kill bacteria. Thus, the preparation of pharma-inks, the printing of chewable tablets, and the packaging must always be carried out under conditions that ensure a limited risk of contamination.

3.2.4. In-vitro drug dissolution and kinetics

Despite some contradictory findings in the literature, Sulfamethoxazole (SMX) and Trimethoprim (TMP) are generally classified as Biopharmaceutics Classification System (BCS) Class II molecules (Takagi

Table 2
Comparison of sensory scores from 6 volunteers (N = 6), for two formulations (gummy vs suspension) using the Wilcoxon rank sum test. Each of the 6 volunteers evaluated both formulations, resulting in 12 observations per sensory attribute.

Attribute	N	Median rank		Results
		Gummy (N = 6)	Suspension (N = 6)	
Texture	12	3.0	5.0	$F_{1,10} = 20.00$, $p < 0.01$
Sweetness	12	3.0	3.0	$F_{1,10} = 0.38$, $p = 0.55$
Immediate bitterness	12	4.0	5.0	$F_{1,10} = 0.70$, $p = 0.42$
Lasting bitterness	12	3.5	2.0	$F_{1,10} = 13.89$, $p < 0.01$
Global	12	4.0	3.0	$F_{1,10} = 90.00$, $p < 0.01$

et al., 2006). This classification indicates that their absorption is primarily limited by their low solubility. For a pH around 1.1–1.2 and a temperature of 32 °C, the solubility of Trimethoprim and Sulfamethoxazole is 5.1 mg/mL and 1.5 mg/mL, respectively (Dahlan et al., 1987).

The dissolution behaviour of SMX and TMP is governed by several parameters, including the nature and pH of the dissolution medium, as well as the intricate interplay between the concentrations of each active pharmaceutical ingredient (API) (Dahlan et al., 1987, 1988; Giordano et al., 1995; Medina et al., 2015). Factors such as ionic strength, the presence of excipients, and the physical state of the APIs further influence the dissolution kinetics.

In our study, the dissolution yields of the 100 mg SMX/TMP chewable tablets ranged from 97.1 % to 102 % after one hour, significantly exceeding the 75 % threshold specified in the relevant monograph. This high dissolution yield demonstrates that the gummy formulation effectively facilitates rapid and complete dissolution of the APIs. As shown in Fig. 7, the dissolution profiles of the chewable tablets are comparable to those of the BACTRIM® tablets and oral suspension. Within 15 min, both the chewable tablets and the BACTRIM® tablets achieved dissolution yields of approximately 75 % and reach nearly 100 % dissolution by 30 min. In contrast, the dissolution rate of the APIs in the BACTRIM® oral suspension did not exceed 90 %. This reduced dissolution could be attributed to the precipitation of sodium carmellose at pH levels below 2, which may trap a portion of the active ingredients, limiting their availability in the solution (Rowe et al., 2009).

Similarly, the dissolution profiles for TMP in chewable tablets, suspension and BACTRIM® tablets were closely aligned. All formulations show dissolution yields between 90 to 100 % within the first 15 min, confirming TMP is more soluble than SMX under these conditions.

To evaluate the similarity between different dissolution profiles, the similarity factor (f_2) is commonly used, particularly for BCS Class II molecules that exhibit more than 85 % dissolution within 30 min (Shah et al., 1998; Karalis et al., 2010). The f_2 factor, which is endorsed by both the FDA and EMA, provides a metric to assess bioequivalence between different pharmaceutical formulations (FDA, 2001; EMA, 2010). The f_2 values range from 0 to 100, with values greater than 50 indicating similarity between dissolution profiles.

In our analysis, the f_2 factor was calculated to compare the dissolution kinetics of SMX in the oral suspension and the commercial SMX/TMP tablets. The obtained f_2 value of 99.76 for Sulfamethoxazole and 94.97 for Trimethoprim indicates a high similarity in the dissolution kinetics between these two formulations. However, the f_2 factor could not be applied to other comparisons because the dissolution rates for the chewable tablets exceeded 85 % within 30 min, which limits the utility of the f_2 metric in those cases.

3.3. Stability study

3.3.1. Stability under stress condition

Forced degradation studies are a fundamental component of the drug pre-formulation process, designed to provide essential information on the intrinsic stability of pharmaceutical compounds, whether they are small molecules or biopharmaceutical products. These studies are crucial for simulating the various conditions to which the future drug will be subjected—from preparation to usage—ensuring the development of a stability-indicating method that allows for continuous monitoring of drug quality over time. In doing so, the primary objective of these studies is to rapidly gather data on the preparation, handling, storage, and usage conditions that guarantee the drug's efficacy and safety. The significance of these degradation tests is widely described in the literature (Tamizi and Jouyban, 2016). However, despite the existence of a defined regulatory framework (WHO, 2018; EMA, 2023), the expectations for these studies can sometimes lack clarity, leading to varying interpretations and implementations (Zelesky et al., 2023).

In this study, the developed method allowed for an analysis duration of 15 min per sample, with relative retention times of 5 min for Trimethoprim and 10 min for sulfamethoxazole. Additional details on method validation are provided in Supplementary Table S2.

For this work, the conditions used were carefully chosen based on literature recommendations to effectively detect the presence of degradation products (Espinosa dos Santos et al., 2022; St-Jean et al., 2021). The forced degradation tests conducted under these specified conditions did not reveal the formation of degradation products; the concentrations of active ingredients remained stable (variation less than 5 %) between D0, D1 and D2 days.

The literature suggests that while photolysis can indeed trigger the degradation of both APIs (Abellán et al., 2009; Cai and Hu, 2017), it does not seem to produce any toxic degradation products (Borowska et al., 2019). Nevertheless, due to the absence of photolysis testing in this study, the stability evaluation was conducted under conditions specifically designed to eliminate the risk of this type of degradation.

3.3.2. Pharma-ink stability

Pharma-inks were evaluated over a three-month period under two

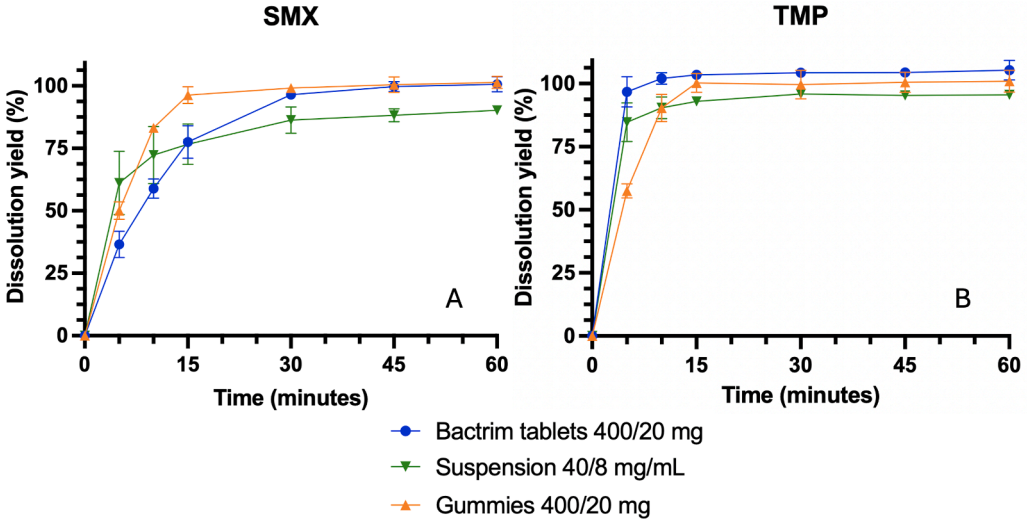

Fig. 7. Comparison of dissolution yields of commercial BACTRIM® (400/80 mg) tablets, SMX/TMP (400/80 mg) chewable tablets after 24 h of drying and BACTRIM® (40/8 mg/mL) suspension over time intervals of 0, 5, 10, 15, 30, 45, and 60 min. The data are presented as mean dissolution yields with standard deviations indicated by error bars. Panel A illustrates the dissolution of SMX, while Panel B details TMP dissolution. The results shown are mean ± SD (N = 12).

storage conditions: room temperature (20–25 °C) and refrigeration (2–8 °C) for chemical and physical stability. Insights into the physical and chemical stability of the chewable tablets and ink over time, focusing on both storage conditions (room temperature and refrigerated), are provided in Fig. 8.

Over time (D0, D30, D45, D60, D90), inks stored at room temperature exhibited increasing storage modulus (G') and tan(δ) values (Fig. 8**A**). This was extensively discussed in section 3.1.2, where it was established that storage at room temperature quickly leads to the inks becoming unprintable. At around 3 months, slight aggregation was noted in syringes stored at room temperature. This phenomenon may be explained by lower cross-linking of gelatine at ambient temperatures, leading to increased mobility within the syringe (Darji et al., 2018).

By contrast, Fig. 8**B** shows that when the ink is stored between 2–8 °C the variation in G' over time is markedly lower. Refrigeration thus significantly slows the hardening process, preserving the ink's original rheological properties. The tan (δ) values under refrigerated conditions remain stable, indicating that the ratio of elastic to viscous characteristics is maintained. Consequently, cold storage extends the period during which the ink remains easily printable and minimizes rheological drift—a phenomenon consistent with known properties of gelatine and similar gelling agents, which retain mechanical strength and gelling capacity better at lower temperatures (Schrieber and Gareis, 2007).

Moreover, HPLC analysis confirmed no significant degradation (≥ 95 % recovery) of SMX/TMP in refrigerated inks over 90 days (Fig. 8**D**), whereas a notable drop in API content (≈ 10 %) was observed at room temperature by D90.

Overall, the recommended storage for pharma-inks is under refrigerated conditions, with a maximum shelf life of 3 months, to maintain both rheological performance and API integrity. This three-month limit ensures minimal rheological drift and preserves API content above acceptable thresholds for therapeutic efficacy.

3.3.3. *Chewable tablet stability*

The physicochemical stability of chewable tablets differs from that of traditional solid dry oral forms. Their hydrogel nature necessitates a partial drying step before packaging, which will not be fully completed. The residual moisture within the tablets represents both an advantage, allowing them to maintain adequate flexibility and palatability, and a disadvantage, as water is known to accelerate degradation processes, particularly through direct hydrolysis of active ingredients.

In this study, packaging the chewable tablets after 24 h of drying at room temperature helped limit the effects of moisture on degradation, although some risk persists (Bouwman-Boer et al., 2015). Throughout the stability study, the chewable tablets showed no notable changes in odour, taste or colour, illustrating their robustness in maintaining

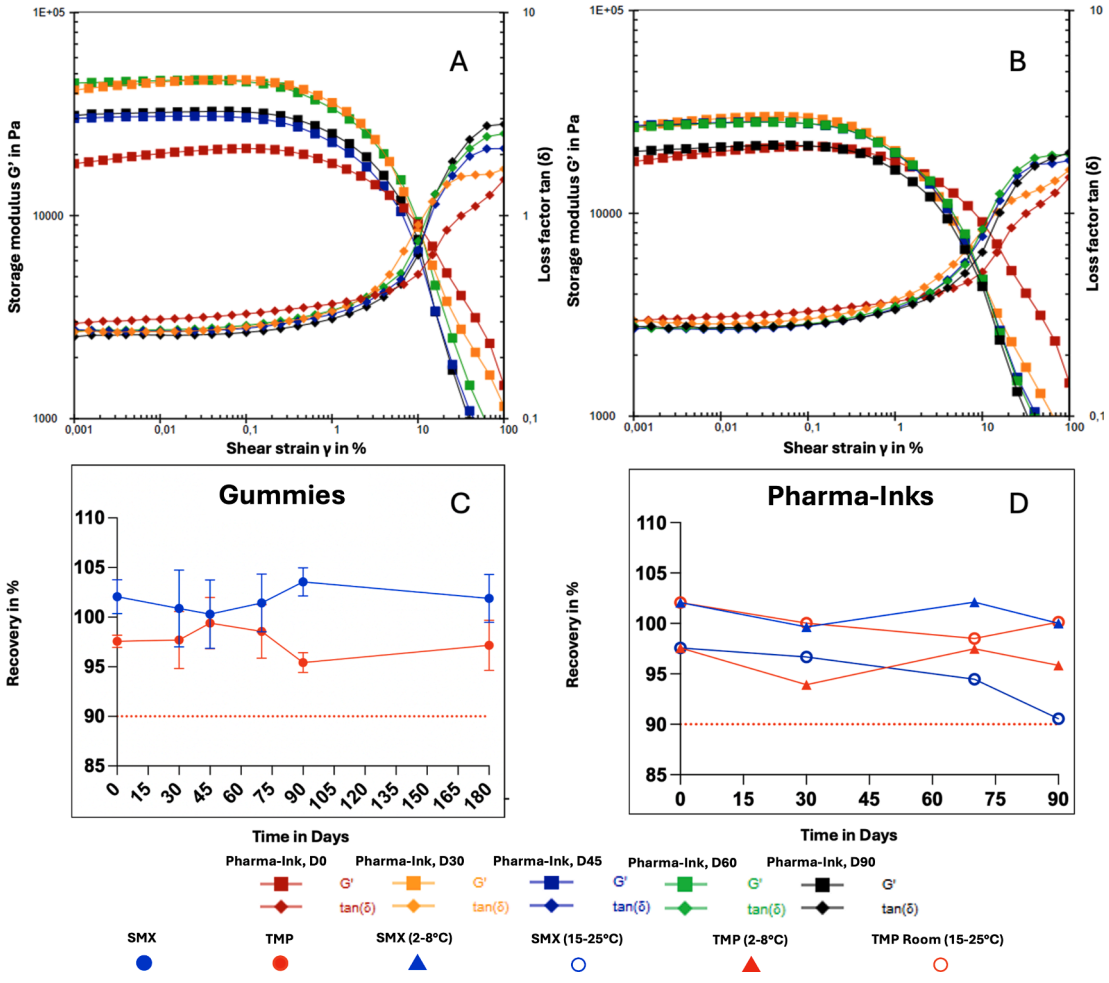

Fig. 8. Physical and chemical stability of chewable tablets and ink. Fig. 8**A**: Evolution of storage modulus (G') and tan(δ) during shear strain (γ) increase for ink store at room temperature at different time points (D0, D30, D45, D60, D90). Fig. 8**B**: Evolution of storage modulus (G') and tan(δ) during shear strain (γ) increase for ink store at fridge at different time points (D0, D30, D45, D60, D90). Fig. 8**C**: Recovery of the theoretical content obtained at different times for the chewable tablets (D0, D30, D45, D60, D90). Fig. 8**D**: Recovery of the theoretical content at different times for the ink in syringes, whether stored at room temperature or refrigerated (D0, D30, D45, D60, D90). The results shown are mean ± SD (N = 3) for API content. Rheological measurements were performed without replicates, at the indicated time points.

organoleptic properties. Insights into API content stability are illustrated in Fig. 8**C**. The data reveal that the theoretical active pharmaceutical ingredient (API) content remained stable over the 180-day period ($\geq$ 95 % recovery). Among various packaging materials, PET bottles kept under refrigeration were ultimately chosen, as they limited water loss to under 1 % after 180 days. Storage conditions also strongly affected mouthfeel: tablets stored at room temperature hardened and became more friable due to continued water evaporation but also increased the brittleness of the tablets, making them more prone to crumbling during handling. Whereas refrigeration preserved both chewability and flavour retention, making it the preferred storage condition. This finding suggests that the formulation, coupled with appropriate packaging, effectively protects the APIs from environmental factors.

In conclusion, refrigerated storage (2–8 °C) effectively preserves both pharma-inks and chewable tablets, maintaining printability, mechanical properties, texture, taste masking and API stability over three months for the pharma-inks and 6 months for the gummies.

4. Conclusion

Two types of 3D-printed chewable formulations incorporating SMX/TMP for paediatric patients were manufactured by SSE technology. The printing process demonstrated high repeatability, yielding consistent mass uniformity in a hospital setting for clinical implementation in a cancer hospital for monolayer chewable tablets. The pharma-inks met the stability requirement, and they were printable over three months. Drug dissolution studies confirmed an immediate release profile comparable to existing commercial formulations, suggesting potential bioequivalence.

Regarding bilayer tablet technology, while it has potential in taste masking by reducing co-localization of the active ingredients, it remains an exploratory approach that requires further optimization for reproducibility, scalability and regulatory compliance before it can be considered for widespread clinical use. Future work should focus on refining the bilayer printing process and evaluation of long-term stability and patient adherence under real-world conditions.

Additionally, the improved palatability compared to traditional oral suspensions addresses a critical barrier to adherence in paediatric patients, making the formulation clinically viable. Clinical feedback from patients who could no longer tolerate commercial forms has been encouraging, underscoring the formulation's utility in addressing unmet medical needs. This work highlights the potential of 3D printing to deliver personalized, on-demand medications, particularly for vulnerable populations like children.

CRediT authorship contribution statement

Maxime Stoops: Writing – original draft, Investigation, Formal analysis. **Bernard Do:** Writing – review & editing, Supervision. **Stéphanie Ramos:** Software, Investigation, Formal analysis. **Bing Xun Tan:** Validation, Investigation, Formal analysis. **Nicholas Yong Sheng Chua:** Supervision, Project administration. **Roseline Mazet:** Writing – review & editing, Resources, Data curation. **Nicolas Guiblin:** Validation, Software, Formal analysis. **Alexandre Michelet:** Writing – review & editing, Software, Formal analysis. **Stephen Flynn:** Resources, Project administration. **Samuel Abbou:** Writing – review & editing, Visualization. **Alvaro Goyanes:** Writing – review & editing, Visualization, Validation. **André Rieutord:** Supervision, Resources. **François-Xavier Legrand:** Writing – review & editing, Writing – original draft, Investigation, Data curation. **Maxime Annereau:** Writing – review & editing, Supervision, Methodology, Conceptualization.

Declaration of competing interest

The authors declare the following financial interests/personal relationships which may be considered as potential competing interests: Bing Xun Tan, Nicholas Yong Sheng Chua, Stephen Flynn works for roquette which give us the excipient for the research. For other authors, they declare that they have no known competing financial interests or personal relationships that could have appeared to influence the work reported in this paper.

Acknowledgements

This research was supported by Roquette Frères (Lestrem, France) by providing the necessary excipients for the developed formulation

Appendix A. Supplementary material

Supplementary data to this article can be found online at https://doi.org/10.1016/j.ijpharm.2025.125581.

Data availability

Data will be made available on request.

References

Abellán, M.N., Giménez, J., Esplugas, S., 2009. Photocatalytic degradation of antibiotics: The case of sulfamethoxazole and trimethoprim. Catal. Today. 144 (1–2), 131–136.
Agafonova, E.V., Moshchenskii, Y.V., Tkachenko, M.L., 2013. Determining the thermodynamic melting parameters of sulfamethoxazole, trimethoprim, urea, nicodin, and their double eutectics by differential scanning calorimetry. Russ. Chem. A Eur. J. 87 (8), 1291–1294.
Alessandrini, E., Gonakova, M., Batchelor, H., Gizurarson, S., Iurian, S., Klein, S., et al., 2023. Colour of medicines and children's acceptability? a systematic literature review of children's perceptions about colours of oral dosage forms. Pharmaceutics 15 (7), 1992.
Algahtani, M.S., Mohammed, A.A., Ahmad, J., Abdullah, M.M., Saleh, E., 2021. 3D printing of dapagliflozin containing self-nanoemulsifying tablets: formulation design and in vitro characterization. Pharmaceutics 13 (7), 993.
Alsubaie, M., Aljohani, M., Erxleben, A., McArdle, P., 2018. Cocrystal forms of the BCS class IV drug sulfamethoxazole. Cryst. Growth Des. 18 (7), 3902–3912.
Andreazza, R., Morales, A., Pieniz, S., Labidi, J., 2023. Gelatin-based hydrogels: potential biomaterials for remediation. Polymers 15 (4), 1026.
Annereau, M., Toussaint, B., Dufaÿ Wojcicki, A., Dufaÿ, S., Diaz Salmeron, R., Boudy, V., 2021. 2D-3D printing in hospital pharmacies, what roles and challenges? Ann. Pharm. Fr. 79 (4), 361–374.
Azad, M.A., Olawuni, D., Kimbell, G., Badruddoza, A.Z.M., Hossain, M.S., Sultana, T., 2020. Polymers for extrusion-based 3D printing of pharmaceuticals: a holistic materials-process perspective. Pharmaceutics 12 (2), 124.
Baguley, D., Lim, E., Bevan, A., Pallet, A., Faust, S.N., 2012. Prescribing for children – taste and palatability affect adherence to antibiotics: a review. Arch. Disease Childhood 97 (3), 293–297.
Basit, A.W., Gaisford, S. (Eds.), 2018. 3D Printing of Pharmaceuticals. Springer International Publishing, Cham.
Binson, G., Sanchez, C., Waton, K., Chanat, A., Di Maio, M., Beuzit, K., et al., 2021. Accuracy of dose administered to children using off-labelled or unlicensed oral dosage forms. Pharmaceutics 13 (7), 1014.
Borowska, E., Gomes, J.F., Martins, R.C., Quinta-Ferreira, R.M., Horn, H., Gmurek, M., 2019. Solar photocatalytic degradation of sulfamethoxazole by TiO_2 modified with noble metals. Catalysts 9 (6), 500.
Bouwman-Boer, Y., Fenton-May, V., Le Brun, P., 2015. In: Practical pharmaceutics: An international guideline for the preparation, care and use of medicinal products. Springer, Cham.
Cai, Q., Hu, J., 2017. Decomposition of sulfamethoxazole and trimethoprim by continuous UVA/LED/TiO_2 photocatalysis: decomposition pathways, residual antibacterial activity and toxicity. J. Hazard. Mater. 323, 527–536.
Carou-Senra, P., Rodríguez-Pombo, L., Monteagudo-Vilavedra, E., Awad, A., Alvarez-Lorenzo, C., Basit, A.W., et al., 2023. 3D printing of dietary products for the management of inborn errors of intermediary metabolism in pediatric populations. Nutrients 16 (1), 61.
Cerveto, T., Denis, L., Stoops, M., Lechanteur, A., Jérôme, C., Leenhardt, J., et al., 2024. The promising role of semi-solid extrusion technology in custom drug formulation for pediatric medicine. Int. J. Bioprinting 10 (6), 4063.
Chatzitaki, A.T., Mystiridou, E., Bouropoulos, N., Ritzoulis, C., Karavasili, C., Fatouros, D.G., 2022. Semi-solid extrusion 3D printing of starch-based soft dosage forms for the treatment of paediatric latent tuberculosis infection. J. Pharm. Pharmacol. 74 (10), 1498–1506.
Chen, H., Xie, F., Chen, L., Zheng, B., 2019. Effect of rheological properties of potato, rice and corn starches on their hot-extrusion 3D printing behaviors. J. Food Eng. 244, 150–158.
Clapham, D., Belissa, E., Inghelbrecht, S., Pensé-Lhéritier, A.M., Ruiz, F., Sheehan, L., et al., 2023. A guide to best practice in sensory analysis of pharmaceutical formulations. Pharmaceutics 15 (9), 2319.

Dahlan, R., Mcdonald, C., Sunderland, V.B., 1987. Solubilities and intrinsic dissolution rates of sulphamethoxazole and trimethoprim. J. Pharm. Pharmacol. 39 (4), 246–251.
Dahlan, R., McDonald, C., Sunderland, V.B., 1988. Dissolution rates of Thrimethoprim-Sulfamethoxazole tablets in aqueous media. Drug Dev. Ind. Pharm. 14 (8), 1125–1129.
Darji, M.A., Lalge, R.M., Marathe, S.P., Mulay, T.D., Fatima, T., Alshammari, A., et al., 2018. Excipient stability in oral solid dosage forms: a review. AAPS Pharm. Sci. Tech. 19 (1), 12–26.
de Moura Oliveira, C.H., Melo de, C.C., Doriguetto, A.C., 2019. Sulfamethoxazole salts: crystal structures, conformations and solubility. New J. Chem. 43 (26), 10250–10258.
de Oliveira Barros, M., Mattos, A.L.A., de Almeida, J.S., de Freitas, R.M., de Brito, E.S., 2023. Effect of ball-milling on starch crystalline structure, gelatinization temperature, and rheological properties: towards enhanced utilization in thermosensitive systems. Foods 12 (15), 2924.
Díaz-Torres, E., Rodríguez-Pombo, L., Ong, J.J., Basit, A.W., Santoveña-Estévez, A., Fariña, J.B., et al., 2022. Integrating pressure sensor control into semi-solid extrusion 3D printing to optimize medicine manufacturing. Int. J. Pharm. X 4, 100133.
Djagny, V.B., Wang, Z., Xu, S., 2001. Gelatin: a valuable protein for food and pharmaceutical industries: review. Crit. Rev. Food Sci. Nutr. 41 (6), 481–492.
Douroumis, D., 2007. Practical approaches of taste masking technologies in oral solid forms. Expert Opin. Drug Deliv. 4 (4), 417–426.
European Society for Paediatric Gastroenterology, Hepatology and Nutrition (ESPGHAN), 2014. 2014 guidelines for the management of acute gastroenteritis in children in Europe. http://www.espghan.org/knowledge-center/publications/Gastroenterology/2014_Guidelines_for_the_Management_of_Acute_Gastroenteritis_in_children_in_Europe (Accessed 6 August 2024).
Espinosa dos Santos, P., Serrou do Amaral, M., Kassab, N.M., 2022. Simultaneous determination of sulfamethoxazole, trimethoprim and bromhexine in veterinary formulation using high performance liquid chromatography (HPLC). Rev. Colomb. Cienc Quím-Farm 51 (1), 293–315.
European Directorate for the Quality of Medicines & HealthCare (EDQM), 2024. 11ème Édition de la Pharmacopée Européenne. https://www.edqm.eu/fr/european-pharmacopoeia-ph-eur.-11th-edition (Accessed 6 August 2024).
European Medicines Agency (EMA), 2010. Investigation of bioequivalence - Scientific guideline. https://www.ema.europe.eu/en/investigation-bioequivalence-scientific-guideline (Accessed 6 August 2024).
European Medicines Agency (EMA), 2013. Pharmaceutical development of medicines for paediatric use - Scientific guideline. https://www.ema.europa.eu/en/pharmaceutical-development-medicines-paediatric-use-scientific-guideline (Accessed 6 August 2024).
European Medicines Agency (EMA), 2023. Stability testing of existing active substances and related finished products - Scientific guideline. https://www.ema.europe.eu/en/stability-testing-existing-active-substances-related-finished-products-scientific-guideline (Accessed 6 August 2024).
Fernandes, N.S., Carvalho Filho, M.A.d.S., Mendez, R.A., Ionashiro, M., 1999. Thermal decomposition of some chemotherapic substances. J. Braz. Chem. Soc. 10 (6), 459–462.
Ferry, J.D., 1980. Viscoelastic Properties of Polymers, third ed. John Wiley & Sons, New-York.
Flammer, L.J., Ellis, H., Rivers, N., Caronia, L., Ghidewon, M.Y., Christensen, C.M., et al., 2024. Topical application of a P2X2/P2X3 purine receptor inhibitor suppresses the bitter taste of medicines and other taste qualities. Br. J. Pharmacol. 181 (17), 3282–3299.
Food and Drug Administration (FDA), 2001. Statistical approaches to establishing bioequivalence. https://www.fda.gov/regulatory-information/search-fda-guidance-documents/statistical-approaches-establishing-bioequivalence (Accessed 6 August 2024).
Gillet, Y., Lorrot, M., Minodier, P., Ouziel, A., Haas, H., Cohen, R., 2023. Antimicrobial treatment of skin and soft tissue infections. Infect. Dis. Now 53 (8S), 104787.
Giordano, F., Bettinetti, G., Cursano, R., Rillosi, M., Gazzaniga, A., 1995. A physicochemical approach to the investigation of the stability of trimethoprim-sulfamethoxazole (co–trimoxazole) mixtures for injectables. J. Pharm. Sci. 84 (10), 1254–1258.
Gutiérrez-López, G.F., Alamilla-Beltrán, L., del Pilar Buera, M., Welti-Chanes, J., Parada-Arias, E., Barbosa-Cánovas, G.V., 2015. Water stress in biological, chemical, pharmaceutical and food systems. Springer, New-York.
Heitman, T., Day, A.J., Bassani, A.S., 2019. Pediatric compounding pharmacy: taking on the responsibility of providing quality customized prescriptions. Children 6 (5), 66.
Huanbutta, K., Burapapadh, K., Sriamornsak, P., Sangnim, T., 2023. Practical application of 3D printing for pharmaceuticals in hospitals and pharmacies. Pharmaceutics 15 (7), 1877.
International Council for Harmonisation of Technical Requirements for Pharamceuticals for Human Use (ICH), 2003. Q1A(R2) Stability testing of new drug substances and products. https://ich.org/page/quality-guidelines (Accessed 6 August 2024).
International Council for Harmonisation of Technical Requirements for Pharmaceuticals for Human Use (ICH), 2023. Q2(R2) Validation of analytical procedures. https://ich.org/page/quality-guidelines (Accessed 6 August 2024).
International Council for Harmonisation of Technical Requirements for Pharmaceutical for Human Use (ICH), 2006. Q3B(R2) Impurities in new drug products. https://ich.org/page/quality-guidelines (Accessed 6 August 2024).
Juárez-Hernández, J.E., Carleton, B.C., 2022. Paediatric oral formulations: Why don't our kids have the medicines they need? Br. J. Clin. Pharmacol. 88 (10), 4337–4348.
Junnila, A., Mortier, L., Arbiol, A., Harju, E., Tomberg, T., Hirvonen, J., et al., 2024. Rheological insights into 3D printing of drug products: Drug nanocrystal-poloxamer gels for semisolid extrusion. Int. J. Pharm. 655, 124070.
Karalis, V., Magklara, E., Shah, V.P., Macheras, P., 2010. From drug delivery systems to drug release, dissolution, IVIVC, BCS, BDDCS, bioequivalence and biowaivers. Pharm. Res. 27 (9), 2018–2029.
Kardas, P., Dabrowa, M., Witkowski, K., 2021. Adherence to treatment in paediatric patients – results of the nationwide survey in Poland. BMC Pediatr. 21 (1), 16.
Khorasani, M., Edinger, M., Raijada, D., Bøtker, J., Aho, J., Rantanen, J., 2016. Near-infrared chemical imaging (NIR-CI) of 3D printed pharmaceuticals. Int. J. Pharm. 515 (1–2), 324–330.
Kilpeläinen, T., Ervasti, T., Uurasjärvi, E., Koistinen, A., Ketolainen, J., Korhonen, O., et al., 2022. Detecting different amorphous – Amorphous phase separation patterns in co-amorphous mixtures with high resolution imaging FTIR spectroscopy. Eur. J. Pharm. Biopharm. 180, 161–169.
Kojima, H., Kurihara, T., Yoshida, M., Haraguchi, T., Nishikawa, H., Ikegami, S., et al., 2021. A new bitterness evaluation index obtained using the taste sensor for 48 active pharmaceutical ingredients of pediatric medicines. Chem. Pharm. Bull. 69 (6), 537–547.
Le, H., Wang, X., Wei, Y., Zhao, Y., Zhang, J., Zhang, L., 2022. Making polyol gummies by 3D printing: effect of polyols on 3D printing characteristics. Foods 11 (6), 874.
Li, P., Jia, H., Zhang, S., Yang, Y., Sun, H., Wang, H., et al., 2019. Thermal extrusion 3D printing for the fabrication of puerarin immediate-release tablets. AAPS Pharm. Sci. Tech. 21 (1), 20.
Li, J., Duggirala, N.K., Kumar, N.S.K., Su, Y., Suryanarayanan, R., 2022. Design of ternary amorphous solid dispersions for enhanced dissolution of drug combinations. Mol. Pharm. 19 (8), 2950–2961.
Li, J., Li, C., Zhang, H., Gao, X., Wang, T., Wang, Z., et al., 2022. Preparation of azithromycin amorphous solid dispersion by hot-melt extrusion: an advantageous technology with taste masking and solubilization effects. Polymers 14 (3), 495.
Madhi, F., Panetta, L., De Pontual, L., Biscardi, S., Remus, N., Gillet, Y., et al., 2023. Antimicrobial treatment of lower respiratory tract infections in children. Infect. Dis. Now 53 (8S), 104782.
Mattoo, T.K., Shaikh, N., Nelson, C.P., 2021. Contemporary management of urinary tract infection in children. Pediatrics 147 (2), e2020012138.
Medina, R., Miranda, M., Hurtado, M., Domínguez, A.M., Reyes, O., Ruiz-Segura, J.C., 2015. In vitro evaluation of trimethoprim and sulfamethoxazole from fixed-dose combination generic drugs using spectrophotometry: Comparison of flow-through cell and USP paddle methods. Trop. J. Pharm. Res. 14 (11), 2061.
Mennella, J.A., Bobowski, N.K., 2015. The sweetness and bitterness of childhood: Insights from basic research on taste preferences. Physiol. Behav. 152 (Pt B), 502–507.
Mistry, P., Batchelor, H., 2017. on behalf of SPaeDD-UK project (Smart Paediatric Drug Development – UK). Evidence of acceptability of oral paediatric medicines: a review. J. Pharm. Pharmacol. 69 (4), 361–376.
Modigell, M., Pola, A., Tocci, M., 2018. Rheological characterization of semi-solid metals: a review. Metals 8 (4), 245.
M'Barki, A., Bocquet, L., Stevenson, A., 2017. Linking rheology and printability for dense and strong ceramics by direct ink writing. Sci. Rep. 7 (1), 6017.
Nelson, C.P., Hoberman, A., Shaikh, N., Keren, R., Mathews, R., Greenfield, S.P., et al., 2016. Antimicrobial resistance and urinary tract infection recurrence. Pediatrics 137 (4), e20152490.
Panraksa, P., Zhang, B., Rachtanapun, P., Jantanasakulwong, K., Qi, S., Jantrawut, P., 2022. "Tablet-in-Syringe": a novel dosing mechanism for dysphagic patients containing fast-disintegrating tablets fabricated using semisolid extrusion 3D printing. Pharmaceutics 14 (2), 443.
US Pharmacopeia (USP), 2015. Sulfamethoxazole and trimethoprim tablets. https://doi.usp.org/USPNF/USPNF_M79300_01_01.html (Accessed 6 August 2024).
Piana, C., Danhof, M., Della, P.O., 2017. Impact of disease, drug and patient adherence on the effectiveness of antiviral therapy in pediatric HIV. Expert Opin. Drug Metab. Toxicol. 13 (5), 497–511.
Podgorbunskikh, E., Kuskov, T., Rychkov, D., Lomovskii, O., Bychkov, A., 2022. Mechanical amorphization of chitosan with different molecular weights. Polymers 14 (20), 4438.
Rodríguez-Pombo, L., Gallego-Fernández, C., Jørgensen, A.K., Parramon-Teixidó, C.J., Cañete-Ramirez, C., Cabañas-Poy, M.J., 2024. 3D printed personalized therapies for pediatric patients affected by adrenal insufficiency. Expert Opin. Drug Deliv. 1–17.
Romandini, A., Pani, A., Schenardi, P.A., Pattarino, G.A.C., De Giacomo, C., Scaglione, F., 2021. Antibiotic resistance in pediatric infections: global emerging threats, predicting the near future. Antibiotics 10 (4), 393.
Rowe, R.C., Sheskey, P.J., Quinn, M.E., 2009. Handbook of pharmaceutical excipients, sixth ed. Pharmaceutical press, London.
Saito, J., Akabane, M., Komura, M., Nakamura, H., Ishikawa, Y., 2018. Age-appropriate pediatric dosage forms in japan insights into end-user perceptions from an observational cross-sectional survey assessing the acceptability of oral formulation. Ther. Innov. Regul. Sci. 53, 1–17.
Sandle, T., 2016. The importance of water activity for risk assessing pharmaceutical products. J Pharm Microbiol 2, 1–2.
Santer, M., Ring, N., Yardley, L., Geraghty, A.W.A., Wyke, S., 2014. Treatment non-adherence in pediatric long-term medical conditions: systematic review and synthesis of qualitative studies of caregivers' views. BMC Pediatr. 14, 63.
Schrieber, R., Gareis, H., 2007. Gelatine handbook: Theory and industrial practice, First ed. Wiley-VCH Verlag GmbH & Co. KGaA, Weinheim.
Schwiebert, E., Wang, Y., Xi, R., Choma, K., Streiff, J., Flammer, L.J., et al., 2021. Inhibition of bitter taste from oral tenofovir alafenamide. Mol. Pharmacol. 99 (5), 319–327.

Seoane-Viaño, I., Januskaite, P., Alvarez-Lorenzo, C., Basit, A.W., Goyanes, A., 2021. Semi-solid extrusion 3D printing in drug delivery and biomedicine: personalised solutions for healthcare challenges. J. Control. Release 332, 367–389.
Shah, V.P., Tsong, Y., Sathe, P., Liu, J.P., 1998. In vitro dissolution profile comparison–statistics and analysis of the similarity factor, f2. Pharm. Res. 15 (6), 889–896.
Shinotsuka, H., Mizutani, N., Aikawa, S., Kimura, G., 2023. Palatability evaluation of sulfamethoxazole/trimethoprim with sweetener using the two-bottle choice test. Chem. Pharm. Bull. 71 (12), 906–908.
Soares, N., Mitchell, R., McGoff, T., Bailey, T., Wellman, G.S., 2022. Taste perceptions of common pediatric antibiotic suspensions and associated prescribing patterns in medical residents. J. Pediatr. Pharmacol. Ther. 27 (4), 316–323.
St-Jean, I., Friciu, M.M., Monfort, A., MacMahon, J., Forest, J.M., Walker, S., et al., 2021. Stability of extemporaneously compounded suspensions of trimethoprim and sulfamethoxazole in amber plastic bottles and amber plastic syringes. Can. J. Hosp. Pharm. 74 (4), 327–333.
Suárez-González, J., Díaz-Torres, E., Monzón-Rodríguez, C.N., Santoveña-Estévez, A., Fariña, J.B., 2024. Revolutionizing three-dimensional printing: enhancing quality assurance and point-of-care integration through instrumentation. Pharmaceutics 16 (3), 408.
Takagi, T., Ramachandran, C., Bermejo, M., Yamashita, S., Yu, L.X., Amidon, G.L., 2006. A provisional biopharmaceutical classification of the top 200 oral drug products in the United States, Great Britain, Spain, and Japan. Mol. Pharm. 3 (6), 631–643.
Tamizi, E., Jouyban, A., 2016. Forced degradation studies of biopharmaceuticals: Selection of stress conditions. Eur. J. Pharm. Biopharm. J. 98, 26–46.
Ternik, R., Liu, F., Bartlett, J.A., Khong, Y.M., Thiam Tan, D.C., Dixit, T., et al., 2018. Assessment of swallowability and palatability of oral dosage forms in children: report from an M-CERSI pediatric formulation workshop. Int. J. Pharm. 536 (2), 570–581.
The RIVUR Trial Investigators, 2014. Antimicrobial prophylaxis for children with vesicoureteral reflux. N. Engl. J. Med. 370 (25), 2367–2376.
van Haaren, C., De Bock, M., Kazarian, S.G., 2023. Advances in ATR-FTIR spectroscopic imaging for the analysis of tablet dissolution and drug release. Molecules 28 (12), 4705.
van Krevelen, D.W., te Nijenhuis, K., 2009. Properties of polymers: their correlation with chemical structure; their numerical estimation and prediction from additive group contributions. Fourth completely revised edition. Elsevier, Amsterdam.
Walsh, J., Cram, A., Woertz, K., Breitkreutz, J., Winzenburg, G., Turner, R., et al., 2014. Playing hide and seek with poorly tasting paediatric medicines: Do not forget the excipients. Adv. Drug Deliv. Rev. 73, 14–33.
Wang, M., Gong, J., Rades, T., Martins, I.C.B., 2023. Amorphization of different furosemide polymorphic forms during ball milling: Tracking solid-to-solid phase transformations. Int. J. Pharm. 648, 123573.
Wang, S., Chen, X., Han, X., Hong, X., Li, X., Zhang, H., et al., 2023. A review of 3D printing technology in pharmaceutics: technology and applications, now and future. Pharmaceutics 15 (2), 416.
Wedamulla, N.E., Fan, M., Choi, Y.J., Kim, E.K., 2023. Combined effect of heating temperature and content of pectin on the textural properties, rheology, and 3D printability of potato starch gel. Int. J. Biol. Macromol. 253, 127129.
Whistler, R.L., BeMiller, J.N., 2009. Starch: chemistry and technology, Third ed. Academic Press, London.
Wooding, S.P., Ramirez, V.A., 2022. Global population genetics and diversity in the TAS2R bitter taste receptor family. Front. Genet. 13, 952299.
World Health Organization (WHO), 2014. Antimicrobial resistance global report on surveillance : 2014 summary. https://www.who.int/publications/i/item/WHO-HSE-PED-AIP-2014.2 (Accessed 6 August 2024).
World Health Organization (WHO), 2018. TRS 1010 - Annex 10: WHO guidelines on stability testing of active pharmaceutical ingredients and finished pharmaceutical products. https://www.who.int/publications/m/item/trs1010-annex10 (Accessed 4 August 2024).
Yi, S., Xie, J., Chen, L., Xu, F., 2023. Preparation of loratadine orally disintegrating tablets by semi-solid extrusion 3D printing. Curr. Drug Deliv. 20 (6), 818–829.
Zelesky, T., Baertschi, S.W., Foti, C., Allain, L.R., Hostyn, S., Franca, J.R., et al., 2023. Pharmaceutical forced degradation (stress testing) endpoints: a scientific rationale and industry perspective. J. Pharm. Sci. 112 (12), 2948–2964.